POWER SYSTEMS DEVELOPMENT FACILITY

TOPICAL REPORT

GASIFICATION TEST CAMPAIGN TC20

AUGUST 8, 2006 – SEPTEMBER 23, 2006

DOE Cooperative Agreement

DE-FC21-90MC25140

Prepared by:
Southern Company Services, Inc.
Power Systems Development Facility
P.O. Box 1069
Wilsonville, AL 35186
Tel: 205-670-5840
Fax: 205-670-5843
http://psdf.southernco.com

July 2008

DISCLAIMER

This report was prepared as an account of work sponsored by an agency of the United States Government. Neither the United States Government nor any agency thereof, nor any of their employees, nor Southern Company Services, Inc., nor any of its employees, nor any of its subcontractors, nor any of its sponsors or cofunders, makes any warranty, expressed or implied, or assumes any legal liability or responsibility for the accuracy, completeness, or usefulness of any information, apparatus, product, or process disclosed, or represents that its use would not infringe privately owned rights. Reference herein to any specific commercial product, process, or service by trade name, trademark, manufacturer or otherwise, does not necessarily constitute or imply its endorsement, recommendation, or favoring by the United States Government or any agency thereof. The views and opinions of authors expressed herein do not necessarily state or reflect those of the United States Government or any agency thereof.

This report is available to the public from the National Technical Information Service, U.S. Department of Commerce, 5285 Port Royal Road, Springfield, VA 22161. Phone orders are accepted at (703) 487-4650.

ABSTRACT

In support of technology development to utilize coal for efficient, affordable, and environmentally clean power generation, the Power Systems Development Facility (PSDF), located in Wilsonville, Alabama, routinely demonstrates gasification technologies using various types of coal. The PSDF is an engineering scale demonstration of key features of advanced coal-fired power systems, including a Transport Gasifier, a hot gas particulate control device (PCD), advanced syngas cleanup systems, and high-pressure solids handling systems.

This report summarizes the results of the first demonstration of the Transport Gasifier following significant modifications of the gasifier configuration. This demonstration took place during test campaign TC20, occurring from August 8 to September 23, 2006. The modifications proved successful in increasing gasifier residence time and particulate collection efficiency, two parameters critical in broadening of the fuel operating envelope and advancing gasification technology. The gasification process operated for over 870 hours, providing the opportunity for additional testing of various gasification technologies, such as PCD failsafe evaluation and sensor development.

ACKNOWLEDGEMENT

The authors wish to acknowledge the contributions and support provided by various project managers, including Morgan Mosser, Elaine Everitt, and Ron Breault of the Department of Energy, Tim Challand of KBR, and John Wheeldon of the Electric Power Research Institute. The project is sponsored by the U.S. Department of Energy National Energy Technology Laboratory under contract DE-FC21-90MC25140.

TABLE OF CONTENTS

Section ..... Page

Inside Cover
Disclaimer
Abstract
Acknowledgement

List of Figures iii
List of Tables v

1.0 EXECUTIVE SUMMARY 1-1
1.1 PSDF Overview 1-1
1.2 Process Description 1-1
1.3 Major Test Objectives 1-4
1.4 Secondary Test Objectives 1-5
1.5 Report Structure 1-6

2.0 COAL FEED 2-1
2.1 Coal Characteristics 2-1
2.2 Coal Feeder Operation 2-3

3.0 TRANSPORT GASIFIER 3-1
3.1 Gasifier Configuration Modifications 3-1
3.2 Gasifier Operating Parameters 3-2
3.3 Gasifier Performance, Solids Analysis 3-4
3.4 Gasifier Performance, Gas Analysis 3-8
3.5 Gasifier Performance, Parametric Testing 3-12
3.6 Ammonia Injection Testing 3-15
3.6 Post-Test Campaign Inspections 3-16

4.0 SENSOR DEVELOPMENT 4-1
4.1 Real-Time Particulate Monitors 4-1
4.1.1 PCME DustAlert-90 4-1
4.1.2 Process Metrix Process Particle Counter 4-1
4.2 Pressure Differential Indicator Ceramic Inserts 4-4
4.3 Thermowell Inserts 4-5

5.0 PARTICULATE CONTROL DEVICE 5-1
5.1 PCD Particulate Collection Performance 5-1
5.1.1 PCD Inlet Mass Loadings 5-1
5.1.2 PCD Outlet Mass Loadings 5-3
5.1.3 Failsafe Performance Tests 5-5
5.1.4 Filter Element Sealing Issues 5-5
5.2 PCD Solids Analysis 5-5

Section.....Page

5.2.1 Particle Size Distributions..... 5-6
5.2.2 Dustcake Observations and Thickness and Areal Loading Measurements 5-8
5.2.3 Particulate Physical Properties and Chemical Composition..... 5-9
5.2.4 PCD Pressure Drop Performance..... 5-14
5.2.4.1 Transient PCD Drag..... 5-14
5.2.4.2 Baseline Pressure Drop Analysis..... 5-17

5.2.5 Prediction of PCD Drag and Pressure Drop 5-18
5.2.5.1 Lab Drag Measurements..... 5-18
5.2.5.2 Comparison of Lab Measurements with Transient Drag..... 5-20
5.2.6 Analysis of PCD Filter Element Condition 5-22

6.0 ADVANCED SYNGAS CLEANUP..... 6-1
6.1 COS Hydrolysis Testing 6-1
6.2 Syngas Cooler Fouling Testing..... 6-1

7.0 CONCLUSIONS..... 7-1

APPENDIX A OPERATING HISTORY..... A-1

APPENDIX B STEADY STATE OPERATING PERIODS AND MAJOR OPERATING PARAMETERS B-1

APPENDIX C MATERIAL AND ENERGY BALANCES.....C-1

APPENDIX D LIST OF ABBREVIATIONS AND UNITS D-1

LIST OF FIGURES

Figure ..... Page

1-1 PSDF Gasification Process Flow Diagram 1-2

2-1 Coal Particle Sizes 2-2
2-2 Coal Fines and Oversize Particles 2-2
2-3 Average Coal Particle Size Distribution Before and After Mill Adjustments 2-3
2-4 Vent Valve Replacement on Original Coal Feeder 2-4
2-5 Schematic of Original Coal Feeder 2-4
2-6 Coal Feeder Operating Envelope 2-5
2-7 Coal Fines Content versus Coal Moisture Content 2-5

3-1 Gasifier Refractory 3-2
3-2 Gasifier Operating Parameters 3-3
3-3 Air, Nitrogen, Coal, Steam, and Oxygen Flow Rates to Gasifier 3-4
3-4 Standpipe and Riser Differential Pressures 3-4
3-5 Comparison of Gasifier and PCD Solids Compositions 3-6
3-6 Particle Sizes of Gasifier Circulating Solids and PCD Solids 3-6
3-7 Bulk Densities of Gasifier Circulating Solids and PCD Solids 3-7
3-8 Gasification Ash Removal from the Gasifier and PCD 3-8
3-9 Syngas H_2O Concentration versus Steam Flow Rate 3-9
3-10 Carbon Conversion 3-11
3-11 Syngas Lower Heating Value as a Function of Coal Feed Rate 3-12
3-12 Comparison of Gasification Efficiencies versus Coal Rate for TC18, 19, and 20 3-13
3-13 Carbon Conversion as a Function of Gasifier Temperature 3-13
3-14 Gasifier Temperature Differential as a Function of Percent Air Fed to Lower Mixing Zone 3-14
3-15 Circulation Rate as a Function of Standpipe Level 3-15
3-16 Ammonia and NOx Measurements during Ammonia Injection Testing 3-16
3-17 Inspection of the First Solids Separation Device 3-17
3-18 Inspection of the Primary Gas Cooler 3-18
3-19 Inspection of the Atmospheric Syngas Combustor 3-18

4-1 PCME Particulate Monitor Response to Particulate Injection 4-2
4-2 PCME Particulate Monitor Response to Particulate Injection for Several Test Campaigns 4-2
4-3 Changes in PPC Particulate Monitor Output with Sample Flow Rate 4-3
4-4 PPC Particulate Monitor Response to Particulate Injection 4-4
4-5 Measurements of Ceramic-Tipped Pressure Differential Indicators Compared to Standard Pressure Differential Indicators 4-5

5-1 PCD Inlet Particulate Concentration as a Function of Coal Feed Rate 5-3
5-2 PCD Outlet Particulate Concentrations for Recent Gasification Test Campaigns 5-4

Figure ..... Page

5-3 Comparison of Particle Size Distributions from In-Situ Samples 5-7
5-4 Change of Median Particle Diameter with Time 5-7
5-5 Comparison of Particle Size Distributions 5-8
5-6 Effect of Carbon Content on Specific Surface Area of Gasification Ash 5-12
5-7 Change in PCD Drag with Time 5-16
5-8 PCD Transient Drag versus Carbon Content of In-Situ Samples 5-16
5-9 Normalized PCD Pressure Drop 5-17
5-10 Normalized PCD Pressure Drop from TC14 through TC20 5-18
5-11 Lab-Measured Drag as a Function of Particle Size 5-19
5-12 Comparison of PCD Transient Drag with Lab Measurements 5-22
5-13 Pressure Drop versus Face Velocity of Iron Aluminide Filter Element with 8,527 Exposure Hours 5-23
5-14 Pressure Drop versus Face Velocity of Iron Aluminide Filter Element with 1,369 Exposure Hours 5-24
5-15 Pressure Drop versus Face Velocity of Dynalloy HR-160 Filter Element with 1,595 Exposure Hours 5-24

C-1 Mass Balance C-1
C-2 Energy Balance C-2
C-3 Carbon Balance C-2

LIST OF TABLES

Table ..... Page

2-1 PRB As-Fed Coal Characteristics 2-1

3-1 Gasifier Circulating Solids Analysis 3-5
3-2 PCD Solids Analysis 3-5
3-3 Comparison of Gasification Ash Particle Size and Density with PRB Operation Before and After Gasifier Modifications 3-7
3-4 Major Syngas Concentrations and Raw Lower Heating Values 3-9
3-5 Ammonia Injection Tests 3-15

5-1 In-Situ Particulate Measurements 5-2
5-2 Dustcake Thickness and Areal Loading Measurements 5-9
5-3 Physical Properties of In-Situ Samples and Samples Used for Lab Measurements 5-10
5-4 Chemical Composition of In-Situ Samples and Samples Used for Lab Measurements 5-11
5-5 Physical Properties of Dustcake Samples 5-13
5-6 Chemical Composition of Dustcake Samples 5-13
5-7 Transient Drag Determined from PCD Pressure Drop and from Lab Measurements ... 5-15
5-8 Average Drag Values Determined from PCD and Lab Measurements 5-21

6-1 COS Hydrolysis Catalyst Properties and Nominal Operating Parameters 6-1

A-1 Gasification Operating History A-2
B-1 Steady State Operating Periods and Major Operating Parameters B-2

1.0 EXECUTIVE SUMMARY

Test campaign TC20 was the first demonstration of the Power Systems Development Facility (PSDF) gasification process following major gasifier modifications completed in 2006. TC20 occurred from August 8 to September 23, 2006. The Transport Gasifier operated with Powder River Basin (PRB) coal for a total of 870 hours in TC20, 835 hours in air-blown gasification mode and 35 hours with the gasifier operating in oxygen-blown mode. In addition to characterizing operation of the modified gasifier, objectives for the test campaign included further testing of hot gas filter components, coal feeder development, experimentation of ammonia injection to the gasifier, completion of air permit compliance testing, continued testing of instrumentation enhancements, and evaluation of several advanced syngas cleanup sorbents and catalysts.

1.1 PSDF Overview

The PSDF, located near Wilsonville, Alabama, was established to support the U.S. Department of Energy's effort to develop cost-competitive and environmentally acceptable coal-based power generation technologies. This effort promotes fuel diversity—a key component in maintaining national security—while meeting the highest environmental standards. The PSDF is developing environmentally friendly technologies that will allow the continued use of coal, the United States' most abundant and least expensive fuel source.

The PSDF is operated by Southern Company Services. Other project participants currently include the Electric Power Research Institute, KBR (formerly Kellogg Brown & Root), the Lignite Energy Council, and Peabody Energy. The facility is a highly flexible test center where researchers can evaluate innovative power system components on a semi-commercial scale at a low cost. Development of advanced power systems at the PSDF is focused specifically on identifying ways to reduce capital cost, enhance equipment reliability, and increase efficiency while meeting strict environmental standards. Current testing involves pressurized feed systems, gasifier optimization using a variety of fuels, sensor development, hot gas particulate removal, and advanced syngas cleanup.

1.2 Process Description

The PSDF gasification process, shown in Figure 1-1, features key components of an integrated gasification combined cycle (IGCC) plant. These include high pressure solids feed systems; a KBR Transport Gasifier; syngas coolers; a hot gas filter vessel, the particulate control device (PCD); continuous ash depressurization systems developed at the PSDF for ash cooling and removal; a novel piloted syngas burner; a slipstream syngas cleanup unit to test various pollutant control technologies; and a recycle syngas compressor.

The coal used as the gasifier feedstock is processed on site, first crushed and then pulverized to a nominal particle diameter between 250 and 400 microns. Coal may be fed to the gasifier using two systems, the original coal feed system and a secondary coal feed system. The original coal feed system is a lock hopper, horizontal pocket feeder design with a "rotofeed" dispenser. It consists of two pressure vessels, with the coal pressurized in an upper lock vessel and then gravity fed into a dispense vessel, which is always pressurized. The material is fed out of the dispense vessel by the rotofeed dispenser, which is driven by a variable speed electric motor and

delivers the material into the discharge line where it is conveyed by air or nitrogen into the gasifier. The secondary coal feeder is a developmental test unit designed to evaluate different feeder mechanisms. Types of mechanisms that can be tested with this system include auger-style, fluid bed, and a higher pressure rotary feeder. Coal is fed at a nominal rate of 4,000 lb/hr.

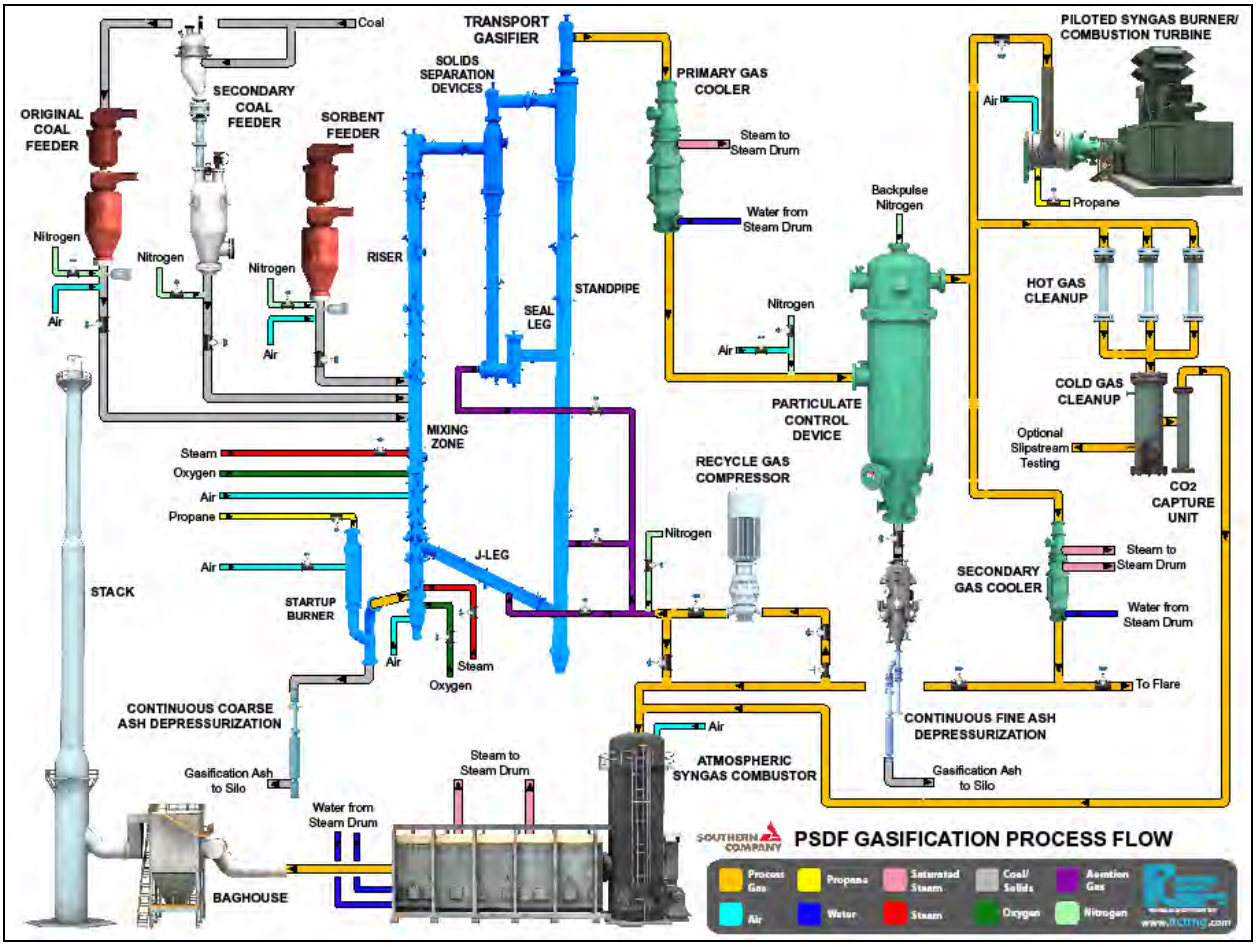

Figure 1-1. PSDF Gasification Process Flow Diagram.

A sorbent feeder is available to feed material into the gasifier for in-situ sulfur capture or to address ash chemistry issues. For sulfur capture, either limestone or dolomite is fed after being crushed and pulverized to a nominal particle diameter of 10 to 100 microns. The sorbent feeder utilizes the same design as the original coal feeder, but for a lower feed rate of nominally 100 lb/hr.

The start-up burner is a direct propane-fired burner operated to heat the gasifier to about 1,200^{o}F. The burner is typically started at a system pressure of 60 psig, and can operate at pressures up to 135 psig.

The Transport Gasifier, a pressurized, advanced circulating fluidized bed reactor, consists of a mixing zone, riser, solids separation unit, seal leg, standpipe, and J-leg. The gasifier is equally capable of using air or oxygen as the gasification oxidant. Steam and either air or oxygen are mixed together and fed into the mixing zone at different elevations and orientations to evenly

distribute heat generated from the partial combustion of the circulating solids. The oxygen from the air or pure oxygen feed is completely consumed in this section of the gasifier. The coal and sorbent are fed at a higher elevation in the mixing zone where the atmosphere is reducing, or oxygen-free.

As the coal devolatilizes and chemical reactions occur to generate syngas, the gas and solids move up the riser and enter the solids separation unit. This unit contains two solids separation devices, which use cyclonic action to remove particles. Between the first and second solids separation devices is the seal leg, which prevents backflow of solids. The solids collected by the solids separation unit are recycled back to the gasifier mixing zone through the standpipe and J-leg. The gasifier solids inventory is controlled by removing gasification ash through the continuous course ash depressurization (CCAD) system, which cools and depressurizes the solids. The nominal gasifier operating temperature is 1,800°F, and the gasifier system was designed to have a maximum operating pressure of 294 psig with a thermal capacity of about 41 MMBtu/hr.

The syngas exits the Transport Gasifier, passes through the primary gas cooler where the gas temperature is reduced to about 750°F, and enters the PCD for final particulate removal. The metal or ceramic filter elements used in the PCD remove essentially all the particulate from the gas stream. The PCD utilizes a tube sheet holding up to 91 filter elements, which are attached to one of two plenums. Process gas flows into the PCD through a tangential entrance, around a shroud, and through the filter elements into the plenums. Failsafe devices are located downstream of the filter elements to stop solids leakage by plugging in the event of element failures. High pressure nitrogen back-pulsing, typically lasting 0.2 seconds, is used to clean the filters periodically to remove the accumulated gasification ash and control the pressure drop across the tube sheet. The solids fall to the bottom of the PCD and are cooled and removed through the continuous fine ash depressurization (CFAD) system.

After exiting the PCD, a small portion of the syngas, up to 100 lb/hr, can be directed to an advanced syngas cleanup system downstream of the PCD. The syngas cleanup system is a specialized, flexible unit, capable of operating at a range of temperatures, pressures, and flow rates, and provides a means to test various pollutant control technologies, including removal of sulfur, nitrogen, chlorine, and mercury compounds. The syngas cleanup slipstream can also be used to test other power generation technologies such as fuel cells.

A portion of the syngas can also be directed to the piloted syngas burner (PSB), a gas turbine combustor designed to burn coal-derived syngas with a lower heating value below 100 Btu/SCF. After syngas combustion in the burner, the flue gas passes through a 4 MWe turbine before exiting the turbine stack. An associated generator can supply power from the turbine to the electric transmission grid.

The main stream of syngas is then cooled in a secondary gas cooler, which reduces the temperature to about 450°F. Some of this gas may be compressed and sent to the gasifier for aeration to aid in solids circulation. The recycle gas compressor is a vertically mounted centrifugal compressor which operates at high temperature, nominally 500 to 600°F, and was designed for a throughput of about 2,000 to 3,000 lb/hr.

The remaining syngas is reduced to near atmospheric pressure through a pressure control valve. The gas is then sent to the atmospheric syngas combustor which burns the syngas components. The flue gas from the atmospheric syngas combustor flows to a heat recovery boiler, through a baghouse, and then is discharged out a stack. A flare is available to combust the syngas in the event of a system trip when the atmospheric syngas combustor is offline.

A brief description of the PSDF gasification testing history can be found in Appendix A.

1.3 Major Test Objectives

Gasifier Modifications. Test campaign TC20 was the initial test campaign following major gasifier modifications, and testing was focused primarily on evaluating these changes. The original design of the Transport Gasifier was based on a combined combustor/gasifier design that limited its performance as a gasifier. In early 2006, changes to the gasifier provided new, more robust solids separation and recycle systems as well as a larger diameter riser. These changes consisted of replacing approximately 85 percent of the existing refractory-lined gasifier. Different types of refractory were installed for evaluation of these materials.

While not precluding future testing in combustion mode, the modifications were designed specifically to enhance performance during gasification operation. The primary goals were to improve the solids collection efficiency and to increase the residence time in the gasifier as well as to demonstrate a solids collection system better suited for commercial scale-up. Increasing the solids collection efficiency should improve the carbon conversion by retaining and recycling more of the carbon solids in the gasifier. Increasing the residence time should also improve the carbon conversion to combustible syngas components.

In the evaluation of the gasifier modifications, parametric testing was conducted and included varying gasifier temperature, pressure, air distribution, riser velocity, and riser density. Testing of the Transport Gasifier performance in oxygen-blown mode was also performed. The system was successfully commissioned and tested with PRB coal, achieving the most stable gasifier operations since gasification testing began, and demonstrating improvements in the solids collection efficiency, syngas heating value, and carbon conversion. Efficiency of the first stage of the gasifier solids separation unit improved significantly, increasing from less than 85 percent to greater than 99 percent. The higher carbon conversion to combustible syngas components increased the raw syngas lower heating value by about 20 percent compared to operation with the previous gasifier configuration. Syngas heating values after the modifications were the highest the PSDF Transport Gasifier had achieved, with the raw lower heating values as high as 87 Btu/SCF on a wet basis and occasionally exceeding 100 Btu/SCF on a dry basis, giving for a power generating commercial plant a projected value of 128 Btu/SCF at the gas turbine inlet.

Particulate Control Device. Because the modifications were expected to impact the PCD particulate characteristics, these effects were evaluated as well. The cyclonic action of the improved gasifier solids collection had the potential to retain the largest particles while allowing smaller particles to pass through. Thus, the size distribution of the particulate was expected to be smaller, which could cause a higher PCD pressure drop. In addition, better solids collection would reduce the total solids mass entering the PCD, which would result in a lower areal loading on the filter elements and potentially lower pressure drop. Testing demonstrated that the particle size distribution did indeed become significantly finer with mass median diameters (MMDs) in

the range of about 6 to 12 microns compared to typical particle size MMD of 15 to 20 microns in previous test campaigns. The improved gasifier particulate collection efficiency resulted in an average PCD inlet mass rate for TC20 that was about 30 percent less than seen in previous test campaigns. Overall, the gasifier modifications did not adversely affect PCD performance.

Additional objectives related to PCD operation were the performance assessment of Dynalloy HR-160 elements and the on-line testing of a new failsafe media configuration. The HR-160 metal fiber filter elements replaced most of the previously tested iron aluminide (FEAL) sintered metal powder elements, and past experience has shown that they are more robust and less prone to breakage than the FEAL elements. Although the collection efficiency of the HR-160 fiber elements has previously been shown to be less than that of the sintered powder elements in cold-flow testing, the HR-160 elements used in TC20 were able to consistently maintain outlet loadings near the lower limit of resolution (~0.1 ppmw). A newly designed HR-160 failsafe, employing a reversed media design for enhanced plugging in the event of filter element failure, showed good results during on-line testing with the valve-activated failsafe tester. A small amount of particle penetration (~ 0.3 ppmw) was measured during the first hour of testing, while testing a day later indicated that the particle penetration rate was below 0.1 ppmw.

1.4 Secondary Test Objectives

Transport Air Evaluation. Air was used as the coal conveying gas, in lieu of the nitrogen typically used, for about 35 percent of the test campaign. Transitioning from nitrogen to air was achieved smoothly, and the use of transport air resulted in a higher syngas heating value.

Ammonia Injection. Anhydrous ammonia was injected into the lower mixing zone to evaluate the effects on gasifier outlet ammonia concentration. The injections resulted in lower mixing zone syngas ammonia concentrations from about one to three times the estimated rate of normal ammonia generation from coal gasification. The gasifier outlet ammonia concentration did not increase due to the ammonia addition, confirming ammonia decomposition in the gasifier.

Air Compliance Testing. Annual air compliance testing was completed, and compliance with the PSDF Title V permit was confirmed.

Coal Feeder Enhancement. A new dispense vessel vent valve reduced the occurrence and severity of vent line plugging in the original coal feeder. Feeder downtime was reduced by over 50 percent compared to the previous test campaign.

Sensor Development. Development continued with real-time particulate monitors, the PCME DustAlert-90 and the Process Metrix Process Particle Counter. Both monitors responded to testing with particulate injection, and modifications needed to improve performance were identified. Evaluation of ceramic-tipped pressure differential indicators (PDIs) was continued, as well as testing of thermowell material for improved gasifier thermocouple longevity. The ceramic tips prevented plugging of solids in the PDI sensing lines, and the instruments compared well with standard PDI measurements. The thermowells functioned well, and there were no thermocouple failures during operations.

Advanced Syngas Cleanup. Testing of syngas cleanup included carbonyl sulfide (COS) hydrolysis with several catalysts. Conversions ranged from 80 to 93 percent.

1.5 Report Structure

The following report presents the operational data and results of gasification technology development at the PSDF during TC20, compiled in the sections listed below.

Section 2 Coal Feed — Presents analysis of the PRB coal used during TC20. Discusses coal feeder modifications and operation of the coal feed systems. Presents coal moisture values and particle sizes and their effects on coal feeder performance.

Section 3 Transport Gasifier — Details gasifier configuration modifications. Includes the major gasifier operating parameters and the gasifier performance as indicated by solids and gas analyses. Also includes the inspection results for the gasifier and related equipment.

Section 4 Sensor Development — Discusses testing of real-time particulate monitors and results of gasifier instrumentation improvements.

Section 5 Particulate Control Device — Describes the hot gas filter particulate characteristics, PCD performance, and failsafe and filter element testing.

Section 6 Advanced Syngas Cleanup — Details testing to support emissions control studies.

Section 7 Conclusions — Lists the major conclusions and lessons learned from TC20 operation.

Appendix A gives a brief history of gasification operation at the PSDF. Appendix B shows the steady state operating periods and the major system operating conditions for each period. Material and energy balances are shown in Appendix C, and Appendix D lists the abbreviations and units used in this report.

2.0 COAL FEED

PRB coal, the most extensively tested fuel at the PSDF, was used exclusively in TC20. Coal feeder technology development continued with the evaluation of coal feeder vent valve modifications incorporated prior to TC20 and with the continued development of the coal feeder operating envelope.

2.1 Coal Characteristics

Characteristics of the PRB coal used during test campaign TC20 were typical of the PRB coal used in previous test campaigns. This feedstock was a blend of coals from Southern Powder River Basin mines, including Jacobs Ranch, Black Thunder, North Antelope/Rochelle, and Antelope mines. Table 2-1 shows the composition and heating values of the coal as sampled from the coal feeders. Hydrogen from the coal is reported separately from hydrogen in the moisture. The as-fed moisture was reduced in the coal mills from typical as-received values of approximately 25 to 30 weight percent.

Table 2-1. PRB As-Fed Coal Characteristics.

	Average	Standard Deviation	Minimum	Maximum
Moisture, wt %	15.9	1.1	13.0	18.0
Carbon, wt %	59.2	0.9	57.4	61.2
Hydrogen, wt %	3.7	0.2	3.2	4.0
Nitrogen, wt %	0.8	0.03	0.7	0.8
Sulfur, wt %	0.3	0.02	0.2	0.3
Ash, wt %	5.4	0.3	4.8	6.5
Oxygen, wt %	14.8	0.6	12.8	16.0
Volatiles, wt %	35.5	2.2	32.9	48.4
Fixed Carbon, wt %	43.2	2.2	30.0	46.8
Higher Heating Value, Btu/lb	9,840	200	8,470	10,290
Lower Heating Value, Btu/lb	9,320	230	7,780	9,790
CaO, wt %	1.2	0.06	1.1	1.4
SiO_2, wt %	1.8	0.2	1.5	2.6
Al_2O_3, wt %	0.9	0.06	0.8	1.0
MgO, wt %	0.3	0.01	0.3	0.3
Na_2O, wt %	0.1	0.01	0.1	0.1
Ca/S, mole/mole	2.8	0.2	2.2	3.2

The mass median diameter (MMD) and Sauter mean diameter (SMD) particle sizes of the coal sampled from the coal feeders are shown in Figure 2-1. The coal particle sizes measured in MMD averaged 251 microns, with a standard deviation of 39 microns, and the coal SMD averaged 168 microns, with a standard deviation of 22 microns.

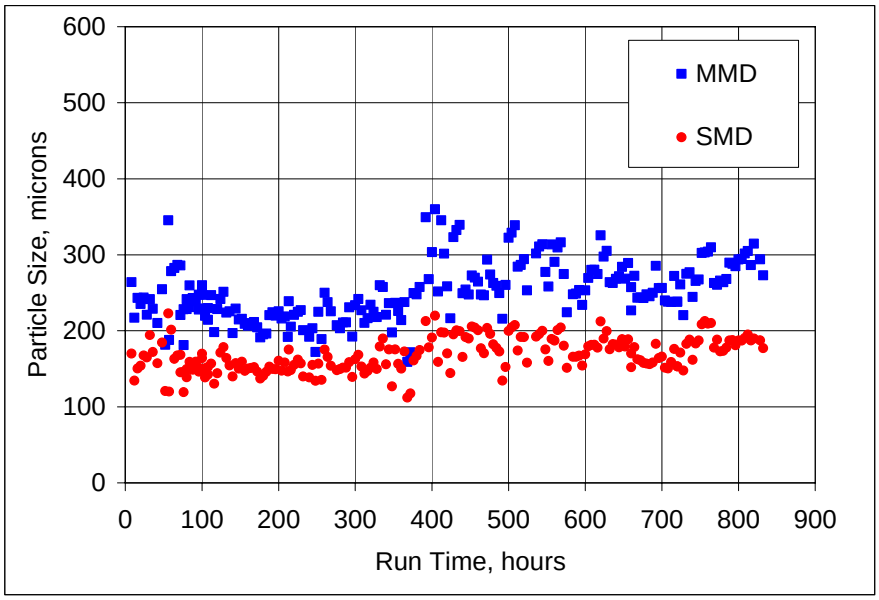

Figure 2-1. Coal Particle Sizes.

Figure 2-2 shows the percentage of fine coal, that below 45 microns, and the percentage above 1,180 microns, considered oversize coal. Fines concentrations were occasionally elevated during the first 400 hours of operation and caused operational problems due to material packing in the lock vessel and plugging in the vent lines. Adjustments were made to the coal mill operating parameters around Hour 400 to increase particle size. Figure 2-3 shows the average particle size distribution curve before and after the adjustments. Overall, the particle size increased and the percentage of fines was reduced. Figure 2-3 shows a shift from left to right in the size distribution curve, although the shape of the curve did not change significantly.

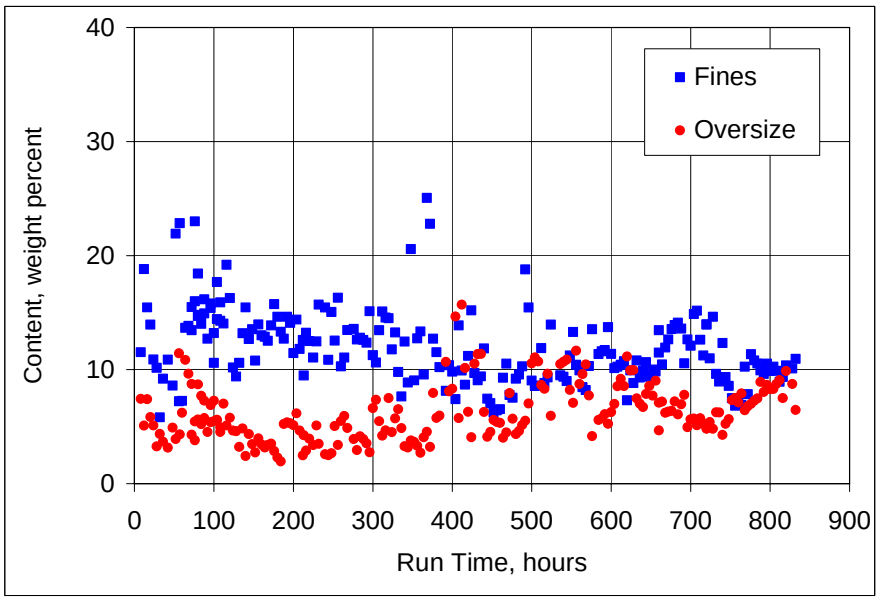

Figure 2-2. Coal Fines and Oversize Particles.

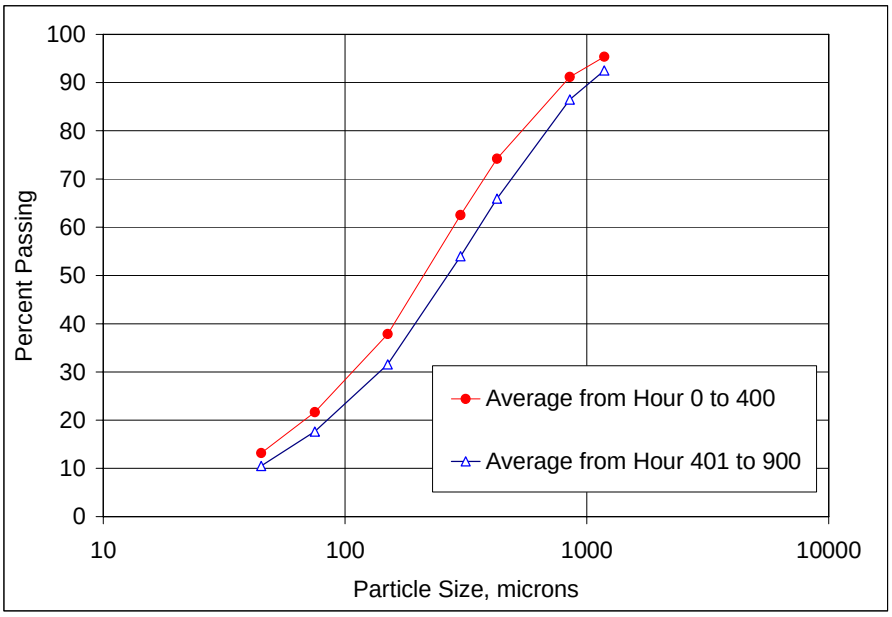

Figure 2-3. Average Coal Particle Size Distribution Before and After Mill Adjustments.

2.2 Coal Feeder Operation

During TC20, both the original feeder and the developmental feeder were used. The original coal feeder operated for a total of 815 hours, achieving rates up to 5,000 lb/hr during high feed rate testing. The Spheri valves on the original feeder cycled over 6,900 times without failure. The developmental feeder functioned as a backup feeder, operating for 108 hours at rates up to 4,400 lb/hr. Discharge line plugging caused periods of operational instability with the developmental feeder.

Vent Valve Modifications. In previous test campaigns, plugging in the vent lines had caused frequent and extensive downtime of the original coal feeder. In TC19, for example, coal feed was interrupted for 20 hours at one point due to complete plugging of the vent lines. To reduce downtime of the original feeder, the two-inch vent valve and associated 7/64-inch flow orifice were removed and replaced with a one-inch ceramic V-ball control valve, which is shown in Figure 2-4. Figure 2-5 shows a schematic of the coal feeder with the location of the new vent valve circled in the figure. Operation of the new dispense vessel vent valve on the original coal feeder resulted in decreased frequency of vent line plugging compared to previous test campaigns. The vent lines plugged occasionally during periods of variability in coal particle sizes, although downtime was limited to less than nine hours in TC20.

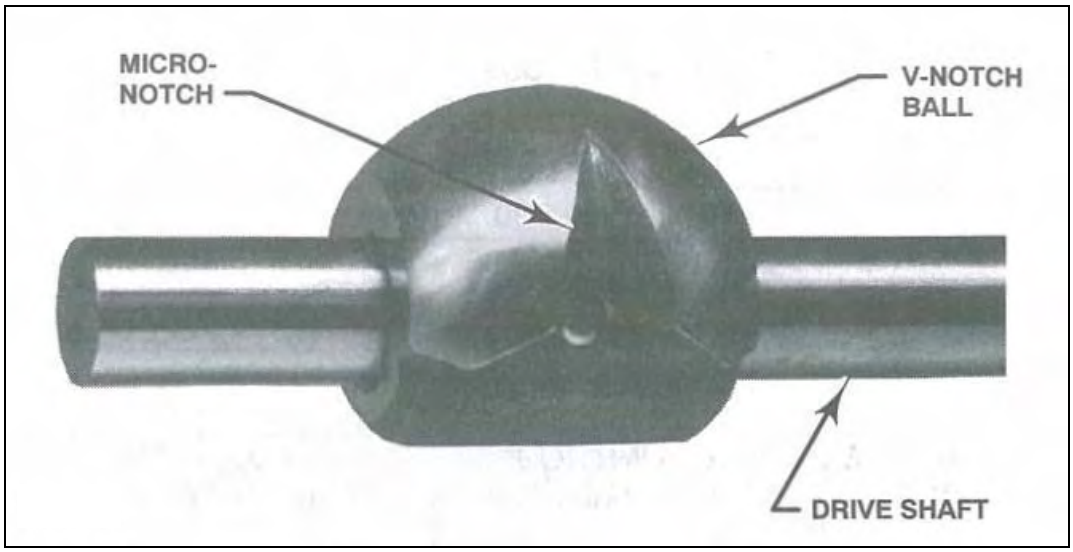

Figure 2-4. Vent Valve Replacement on Original Coal Feeder.

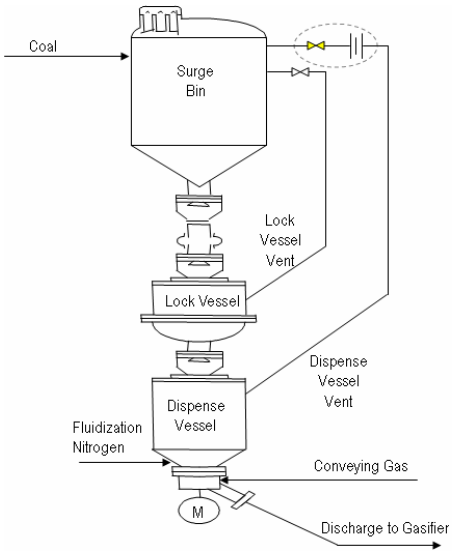

Figure 2-5. Schematic of Original Coal Feeder.

Coal Feeder Operating Envelope. Based on TC20 operations, the original coal feed system operating range for the coal moisture content and particle size was evaluated. Figure 2-6 shows the variation in particle size and coal moisture contents, and the ranges of which were conducive to acceptable feeder operation. Coal feeder operations were problematic when the particle size was less than about 190 microns at a moisture content of about 15 percent. This was due to a high percentage of fines in the feed material as shown in Figure 2-7. During the pressurization step in the coal feeder lock vessel, fine coal particles tend to pack together and do not flow well from the lock vessel into the dispense vessel.

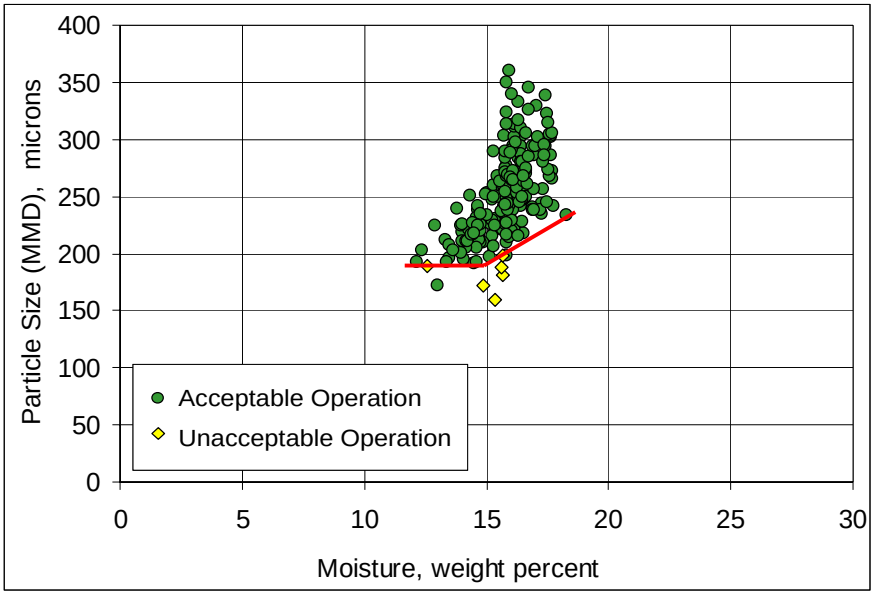

Figure 2-6. Coal Feeder Operating Envelope.

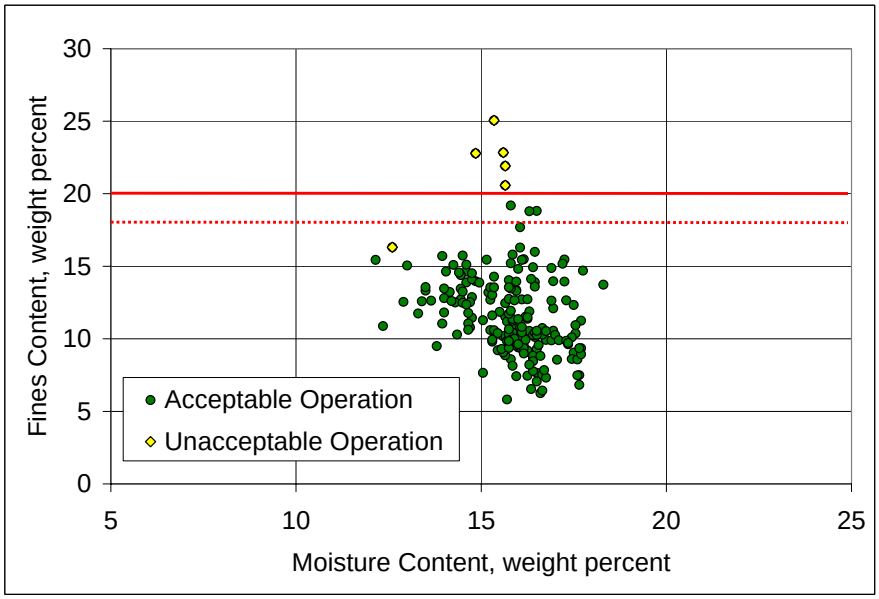

Figure 2-7. Coal Fines Content versus Coal Moisture Content.

3.0 TRANSPORT GASIFIER

Results of the gasifier configuration modifications were evaluated through routine analyses of solids physical and chemical properties, syngas composition, carbon conversion, and syngas heating values at various operating conditions, as well as through parametric studies. In addition to this evaluation, the effect of ammonia injection to the gasifier was tested. Inspections following TC20 were completed to assess the condition of the gasifier and related process equipment.

3.1 Gasifier Configuration Modifications

The gasifier modifications tested in TC20 marked a major effort to improve the performance of the Transport Gasifier while operating with a variety of fuels. The modifications also enhanced the predictability of the scale-up and design of commercial Transport Gasifiers. The changes provided new, more robust solids separation and recycle systems as well as a larger diameter riser and consisted of replacing approximately 85 percent of the refractory-lined gasifier.

With the original design, the particulate laden syngas from the riser passed through a disengager and then into a cyclone before exiting the gasifier. The disengager separated the gas and solids mixture utilizing gravity settlement and operated with about 70 percent collection efficiency. The new design incorporated a two-stage solids separation unit utilizing cyclonic action for both stages of separation. In addition, the solids flow path exiting the second device was improved to eliminate fine gasification ash from packing in the line before flowing back into the standpipe.

The modifications to the solids separation unit were designed to result in higher overall solids capture efficiency. By retaining more carbon containing gasification ash in the gasifier, more solid-phase carbon can be converted into syngas. A higher carbon conversion results in a higher syngas heating value and thus a higher gasification efficiency. This positively impacts the overall process economics. In addition, the higher capture efficiency alleviates the need to add gasifier circulating solids make-up material during normal operation.

Related to scale-up of the disengager, the complex flow field inside the disengager made it difficult to develop a set of design equations that could confidently be used for significant scale-up. If a simple scale-up model which uses the linear velocity in the vessel is utilized, the size of the disengager needed for the commercial process is too large to be economically feasible. Thus, the first stage solids separation device was designed to use cyclonic action.

Erosion was the main concern when using cyclonic action for the first stage separation due to the abrasiveness of the gasification ash and the high solids loading. The design of the first stage device focused on addressing the erosion issues with a design that was scalable to commercial size. Cold flow modeling was performed to develop the design equations based on first principles.

The riser diameter was increased to have the same diameter as the mixing zone. This modification doubled the gas residence time and more than doubled the solids residence time. Increases in the gas and solids residence time should result in a higher first pass carbon conversion. The increase in carbon conversion would result in a lower carbon content in the

gasifier circulating solids which would then result in a higher solids capture efficiency since the solids separation devices have lower collection efficiencies for carbon.

To evaluate different types of refractory, several materials were installed in the various sections of the gasifier based on operating conditions in these sections. Figure 3-1 is a simplified diagram of the gasifier (not an exact representation of the gasifier configuration) which illustrates the locations of the different refractory types. The modified gasifier refractory includes an insulating layer throughout using Resco RS-3A material, which was designed for reducing atmospheres. Prior to the modifications, the hot-face refractory used throughout the gasifier was Resco Resocast 17EC, which features an extended working life. The lower standpipe, which was not modified, contains the original Resocast 17EC material. The largest hot-face portion of the gasifier employs Resco Sureflow 88, an erosion resistant material designed for ease of mixing and replacement. Actchem VC from Vesuvius was utilized in the first solids separation device, and this material features a high corrosion resistance and high coefficient of thermal expansion, although it can be susceptible to cracking. The Plibrico Plicast Hymor 3100 material in the burner leg was selected for its low thermal expansion and thermal shock resistance. Refractory inspections following TC20 and upcoming test campaigns will document material performance.

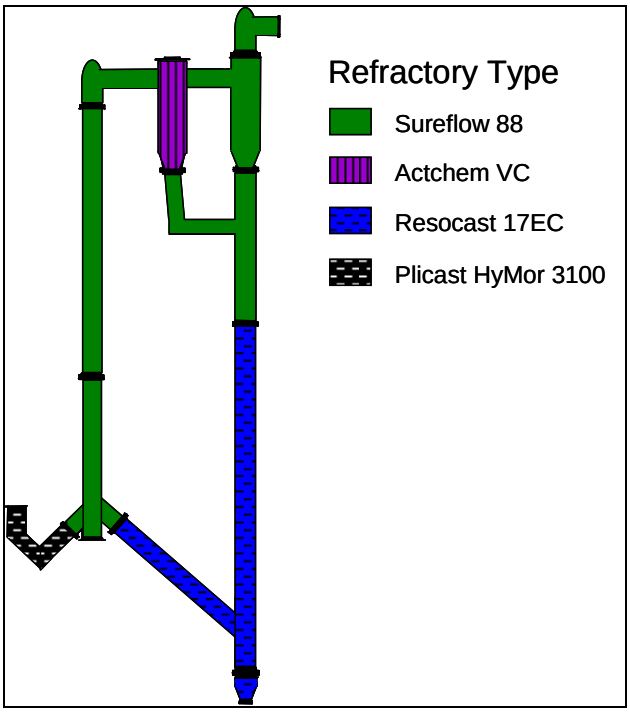

Figure 3-1. Gasifier Refractory.

3.2 Gasifier Operating Parameters

The test campaign consisted of 70 steady state operating periods. The operating periods and major operating parameters are given in Appendix B. The steady state operating periods accounted for approximately 418 hours, or 48 percent of the total TC20 gasification time. All the operating periods consisted of air-blown gasifier operation, except for the last two periods, during which the gasifier operated in oxygen-blown mode. Recycled syngas was not used for

gasifier aeration so that the gasifier modifications could be initially characterized without the added variable of the effect of recycle gas use.

Figure 3-2 gives the gasifier temperatures and pressures for the TC20 steady state periods. The mixing zone temperature varied between about 1,675 and 1,800ºF, and the outlet temperature was between about 1,600 and 1,750ºF. The gasifier outlet pressure, ranging from 140 to 260 psig was frequently varied to characterize the efficiency of the solids separation devices at different gas velocities. During the last two steady state periods, the pressure was lowered to accommodate the limited operating pressure of the oxygen supply system.

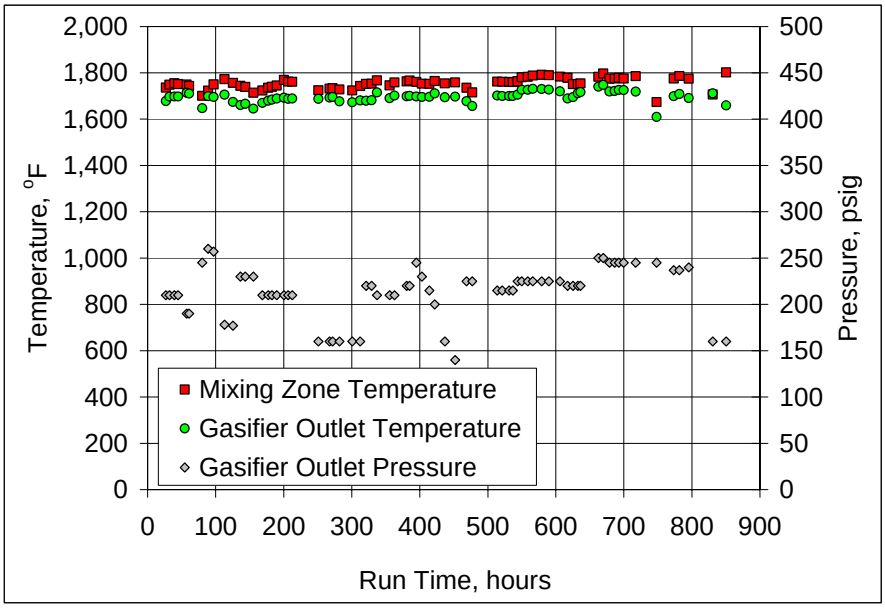

Figure 3-2. Gasifier Operating Parameters.

The air, nitrogen, coal, steam, and oxygen flow rates to the gasifier for the TC20 steady state periods are presented in Figure 3-3. The air and oxygen flow rates shown were rates measured from flow indicators, and the coal feed rates were calculated from the feeder weigh cell output. The nitrogen rates were taken from flow indicators and were adjusted to account for nitrogen used in ash transporting and nitrogen used for coal transport with the secondary coal feeder. The steam flow rates were derived from both the system hydrogen balance and a steam flow indicator.

Figure 3-4 shows the standpipe levels (measured as differential pressures) and the riser differential pressures. The standpipe level was varied to assess the effect of standpipe level on solids circulation rate. The riser differential pressure tracked the standpipe level during most of TC20.

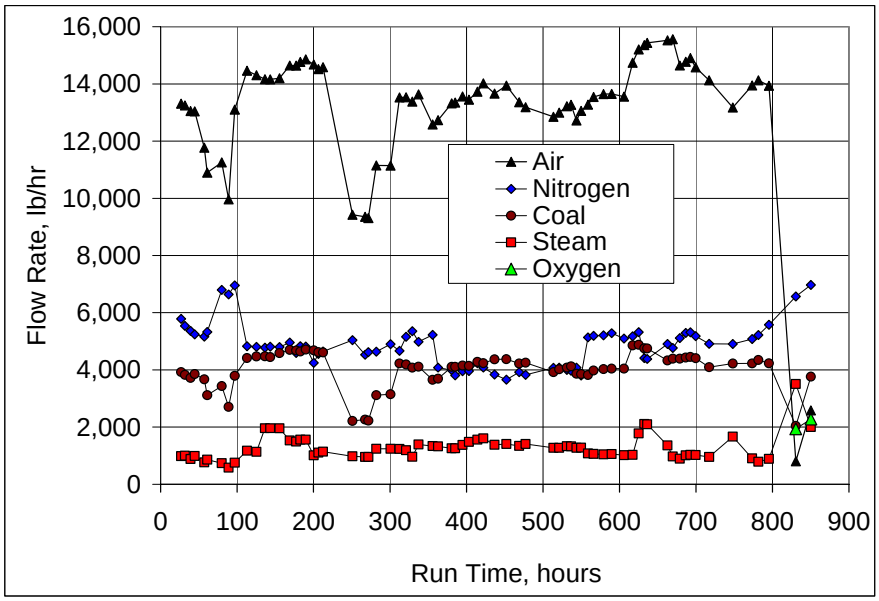

Figure 3-3. Air, Nitrogen, Coal, Steam, and Oxygen Flow Rates to Gasifier.

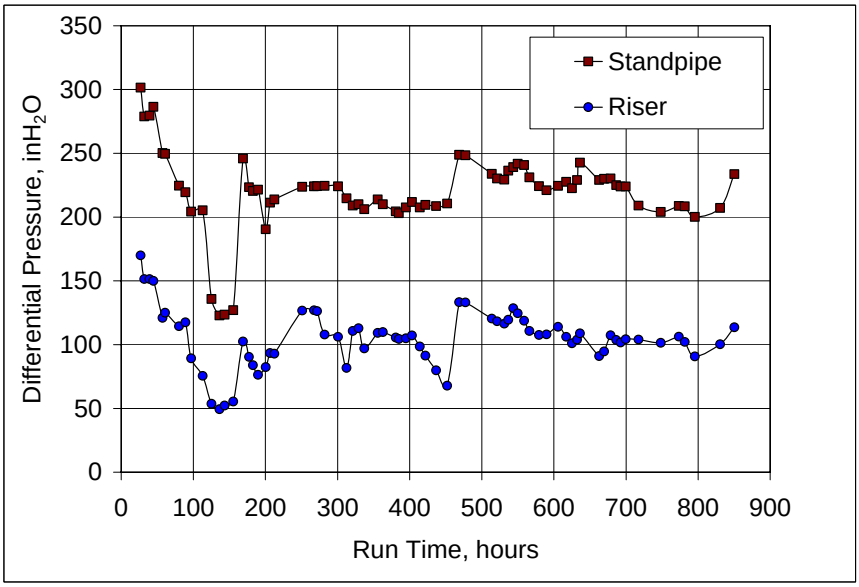

Figure 3-4. Standpipe and Riser Differential Pressures.

3.3 Gasifier Performance, Solids Analysis

The gasifier solids chemical composition and particle size analyses presented in the following sections represent both the circulating gasifier solids sampled from the gasifier standpipe and the solids exiting the gasifier, filtered in the PCD, and sampled from the CFAD ash removal system.

Solids Chemical Analyses. The solids chemical analyses were used in part to characterize operation of the gasifier solids collection devices. The data presented in the chemical analyses represent steady state gasifier solids composition and do not include the five days of operation following initial gasifier startup and the five days following a system restart at Hour 239, which required replacement of gasifier bed material with sand. Sand addition was not required during normal operation as it was during previous test campaigns due to the increased solids collection efficiency of the gasifier.

Table 3-1 gives the chemical analysis of the gasifier circulating solids ash as sampled from the standpipe. The calcium carbonate ($CaCO_3$), calcium sulfide (CaS), and organic carbon contents were negligible in the gasifier solids for most of the steady state periods. The solids analysis including the as-received heating value for the solids captured by the PCD and sampled from the CFAD system is given in Table 3-2.

Table 3.1 Gasifier Circulating Solids Analysis.

	Average	Standard Deviation	Minimum Value	Maximum Value
SiO_2, wt%	41.6	2.9	39.1	52.0
Al_2O_3, wt%	17.8	0.7	15.8	18.8
Other Inerts (BaO, Fe_2O_3, P_2O_5, Na_2O, K_2O, & TiO_2), wt%	11.6	0.9	9.4	12.8
CaO, wt%	22.7	1.3	18.3	24.0
MgO, wt%	5.1	0.4	3.9	5.5

Table 3-2 PCD Solids Analysis.

	Average	Standard Deviation	Minimum Value	Maximum Value
SiO_2, wt%	23.0	3.1	16.5	30.4
Al_2O_3, wt%	12.4	0.8	10.3	14.2
Other Inerts (BaO, Fe_2O_3, P_2O_5, Na_2O, K_2O, & TiO_2), wt%	8.4	0.5	7.2	9.4
$CaCO_3$, wt%	2.4	0.6	0.6	3.9
CaS, wt%	0.9	0.4	0.4	2.2
CaO, wt%	17.4	1.3	14.4	21.3
MgO, wt%	4.7	0.3	4.1	5.4
Organic Carbon, wt%	28.5	4.9	15.3	38.3
Heating Value, As-Recieved, Btu/lb	4,330	760	2,390	5,880

Figure 3-5 compares the silicon dioxide (SiO_2), aluminum oxide (Al_2O_3), calcium oxide (CaO), and organic carbon content of the gasifier circulating solids and PCD solids. The comparison confirms that the gasifier collection efficiency for organic carbon was lower than the overall solids collection efficiency, which resulted in a higher organic carbon concentration in the PCD solids than in the solids remaining in the gasifier.

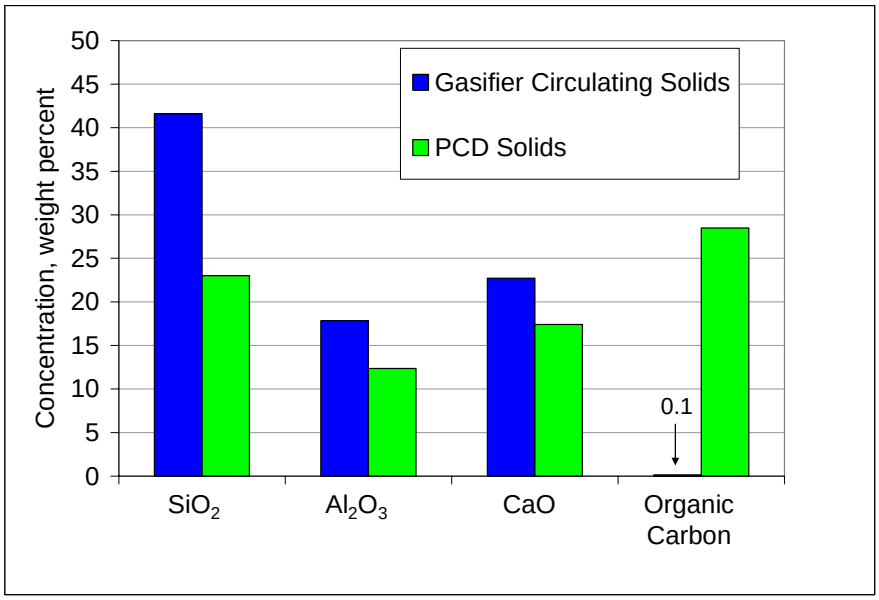

Figure 3-5. Comparison of Gasifier and PCD Solids Compositions.

Solids Physical Analyses. The TC20 particle sizes (measured in SMD) of the gasifier circulating solids and PCD solids are shown in Figure 3-6. The particle size of the circulating solids decreased from 140 to 85 microns SMD during the first 80 hours of TC24 as the start-up sand was replaced with gasification ash. As indicated in the figure, the gasifier solids collection devices were effective in retaining the larger particles, allowing only very fine material of less than 10 microns to flow to the PCD.

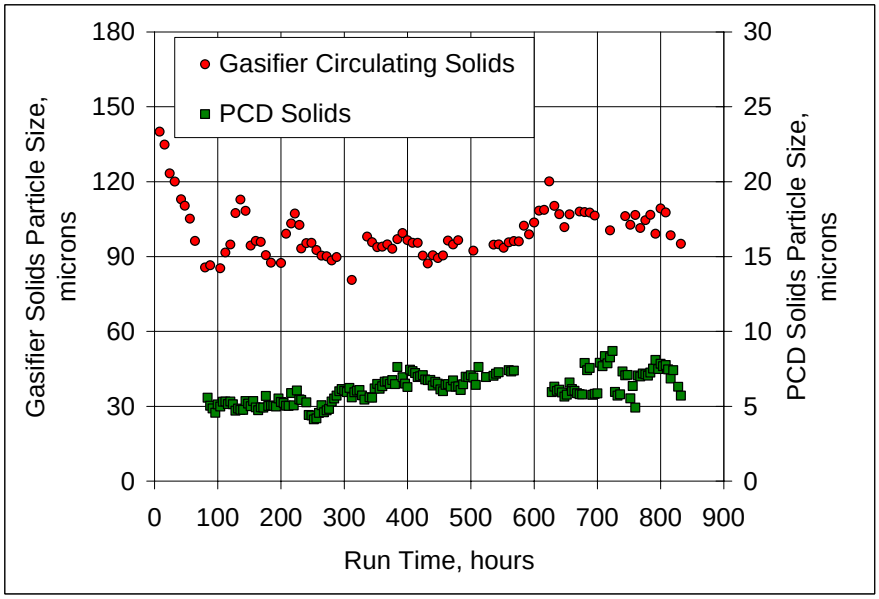

Figure 3-6. Particle Sizes of Gasifier Circulating Solids and PCD Solids.

Bulk densities of the gasifier and PCD solids are plotted in Figure 3-7. The steady state bulk density of the circulating gasifier solids averaged 64.0 lb/ft^3, and that of the PCD solids averaged 14.7 lb/ft^3. The bulk density of the circulating solids decreased from 95 to 60 lb/ft^3 during the first 80 hours of the test campaign as the start-up sand was replaced by gasification ash.

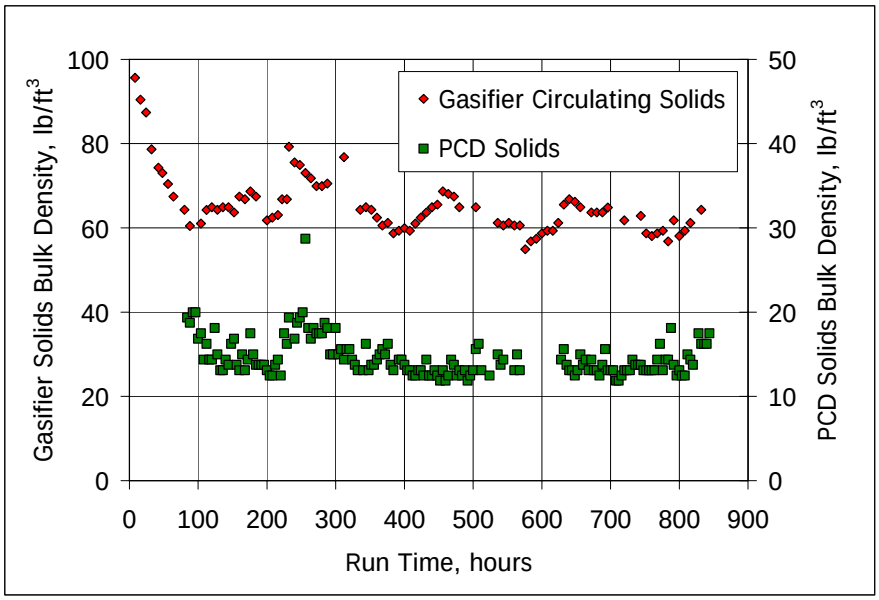

Figure 3-7. Bulk Densities of Gasifier Circulating Solids and PCD Solids.

Table 3-3 shows the maximum and steady state particle sizes and minimum bulk density of the gasifier circulating solids and the average particle size and bulk density of PCD solids for TC20 and all the previous PSDF gasification test campaigns which used PRB coal. As shown in the table, the solids particle sizes and densities decreased significantly following the gasifier configuration modifications. These changes in physical properties after the gasifier modification indicated that the solids collection devices were more efficient in retaining smaller particles than in prior operation. The improved solids retention in the gasifier eliminated the need for occasional addition of relatively high density sand, and the solids density was therefore lower.

Table 3-3. Comparison of Gasification Ash Particle Size and Density with PRB Operation Before and After Gasifier Modifications.

		Gasifier Circulating Solids			PCD Solids	
		Maximum Particle Size (SMD), microns	Steady State Particle Size (SMD), microns	Minimum Bulk Density, lb/ft^3	Average Particle Size (SMD), microns	Average Bulk Density, lb/ft^3
Pre-TC20 PRB Test Campaigns	Average	213	175	79	11	21
	Minimum	156	140	75	8	15
	Maximum	300	230	84	19	28
TC20		140	98	55	6	15

Gasification Ash Removal. Figure 3-8 gives the solids rates for the gasification ash removed from the PCD by the CFAD system and the coarse gasification ash removed from the gasifier standpipe by the CCAD system. The PCD solids rates were determined from the PCD inlet solids concentration (in-situ sampling), and the CCAD rates were determined by a system ash balance. The CFAD system discharged ash from the PCD at rates up to 252 lb/hr, and the CCAD system discharged ash from the gasifier at rates from 34 to 179 lb/hr.

Between 20 and 60 percent of the gasification ash produced was removed by the CCAD system, which was much higher than previous test campaigns with PRB when almost no gasifier solids were removed. In earlier test campaigns, additional solids had to be added in order to maintain the adequate gasifier standpipe levels.

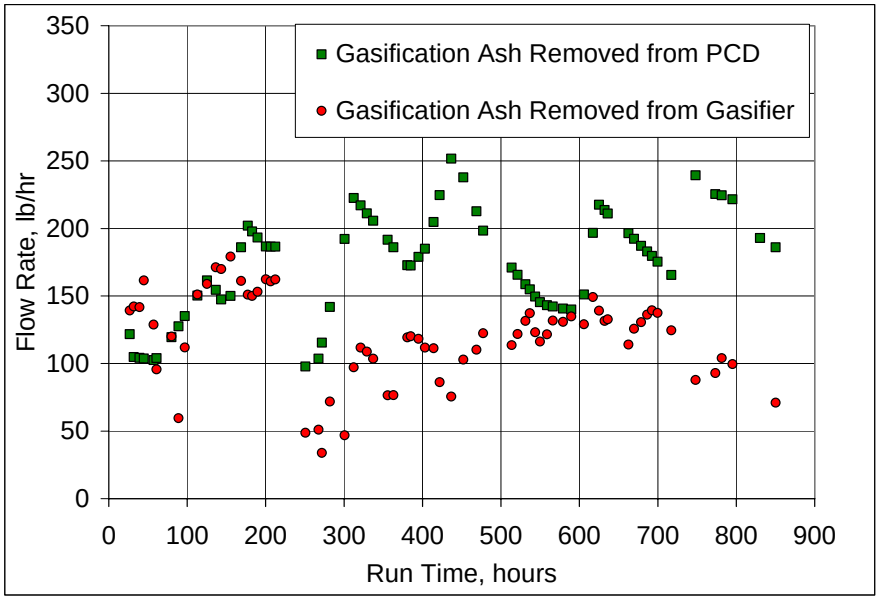

Figure 3-8. Gasification Ash Removal from the Gasifier and PCD.

3.4 Gasifier Performance, Gas Analysis

Continuous extractive syngas sampling was performed between the primary gas cooler and the PCD inlet, and the syngas constituents were analyzed using continuous analyzers and gas chromatography. Other gas analyzers included FTIR (Fourier Transform Infared) analyzers, which measure syngas water (H_2O), ammonia (NH_3), and hydrocarbon concentrations from the advanced syngas cleanup slipstream. Also, in-situ gas analyzers measured the flue gas components from the atmospheric syngas combustor outlet. Manual in-situ samples of syngas moisture were taken at the PCD outlet during the particulate sampling that was used to quantify PCD collection performance.

Syngas Composition. Figure 3-9 shows the H_2O syngas concentrations (derived from water-gas shift calculations) as a function of steam flow rate. The H_2O concentrations ranged from 6.7 to 11.4 mole percent in air-blown operation and were 14.5 and 30.0 mole percent during oxygen-blown operation. As seen in Figure 3-9, the steam flow rate accounted for much of the variation

in H_2O concentration, particularly at higher flow rates. The relationship is not linear since the addition of steam shifts the equilibrium constants of the gasification reactions.

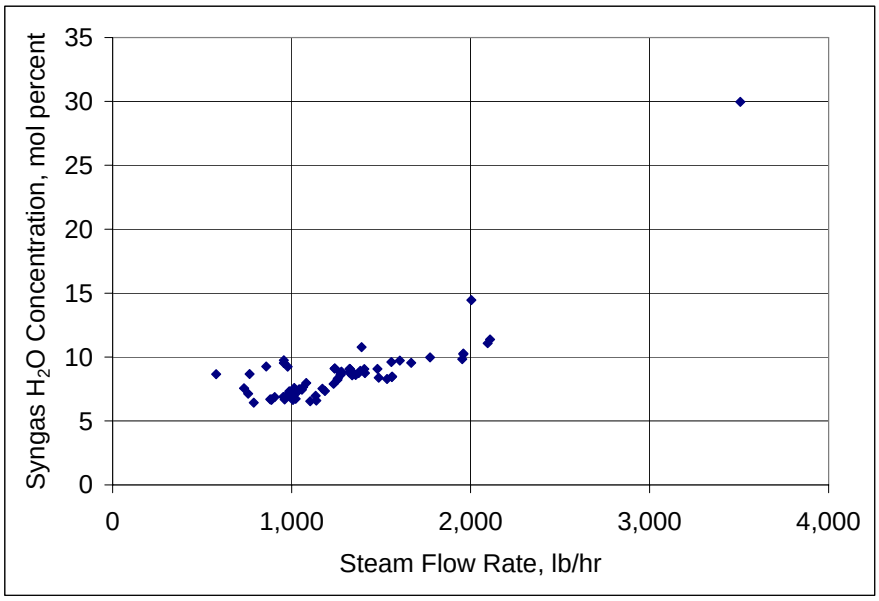

Figure 3-9. Syngas H_2O Concentration versus Steam Flow Rate.

Concentrations of the major syngas components, carbon monoxide (CO), hydrogen (H_2), carbon dioxide (CO_2), and methane (CH_4), as well as the raw syngas lower heating values (LHVs), are shown in Table 3-4. The table gives values that are representative of PSDF design conditions (i.e, periods of relatively high coal feed rates, low steam flow rates, etc.). The balance of the syngas composition was nitrogen less about 0.5 mole percent argon.

Table 3-4. Major Syngas Concentrations and Raw Lower Heating Values.

	Air-Blown			Oxygen-Blown
	Typical Values Achieved under PSDF Design Conditions	Minimum Values	Maximum Values	Typical Values Achieved under PSDF Design Conditions
CO, mol percent	13.5	6.2	13.9	13.1
H_2, mol percent	9.4	5.1	10.4	13.9
CO_2, mol percent	8.4	7.8	9.7	11.7
CH_4, mol percent	1.9	0.6	2	2.2
LHV(wet), Btu/SCF	86.8	39.1	87.4	100.1

Minor constituents in the syngas include reduced sulfur compounds such as hydrogen sulfide (H_2S), carbonyl sulfide (COS), and carbon disulfide (CS_2), and reduced nitrogen compounds such as NH_3 and hydrogen cyanide (HCN). Some of the sulfur (typically less than 15 percent) is captured in the solid phase by forming compounds with the calcium in the coal ash, and the

remaining gas phase sulfur is mostly in the form of H_2S. The H_2S concentration ranged from about 180 to 440 ppm.

A large portion of the coal-bound nitrogen is converted to ammonia. A small number of syngas ammonia measurements were taken due to the limited availability of the FTIR ammonia analyzer. The measurements indicated ammonia concentrations typically ranging from approximately 2,000 to 2,500 ppm during air-blown operation and was slightly higher during the oxygen-blown period due to less nitrogen dilution. The calculated coal nitrogen conversion to ammonia was 80 percent or greater for all periods during which ammonia measurements were available.

The syngas lower heating value was calculated using the following formula:

$$LHV(Btu/SCF) = \frac{275 \times (H_2\%) + 322 \times (CO\%) + 913 \times (CH_4\%)}{100}$$

The raw wet lower heating values, which are presented in Table 3-4, were lower during periods of low coal feed rate and high steam flow rates. The effect of coal feed rate on LHVs is discussed in a subsequent section (Section 3.5). The steam flow rate lowered the raw wet heating values because of the dilution of syngas with moisture, although this effect is eliminated when reporting heating values on a dry basis. The higher syngas heating value, which was achieved during oxygen-blown operation, demonstrated the effect of reduced nitrogen dilution from air. Following the gasifier modifications, the syngas heating value was about 20 percent higher at approximately the same operating conditions.

Carbon Conversion. Carbon conversion is defined as the percent of fuel carbon that is gasified to CO, CO_2, CH_4, and higher hydrocarbons. Carbon in the ash removed is considered a loss, although the heating value from the carbon can be recovered by combusting the gasification ash in a separate process.

Carbon conversion is calculated by dividing the carbon content of the syngas by the total carbon exiting the gasifier (from both solid and gas streams). Figure 3-10 shows the carbon conversion for the steady state operating periods. The carbon conversion ranged from 97.0 to 99.1 percent during PRB operation, averaging 98.0 percent. During the two periods of oxygen-blown operation, the carbon conversion was 97.5 and 98.7 percent. For comparable operating conditions, the carbon conversion for TC20 was higher than for previous PRB test campaigns. The higher carbon conversion was largely a result of the increase in residence time and solids retention resulting from the gasifier modifications.

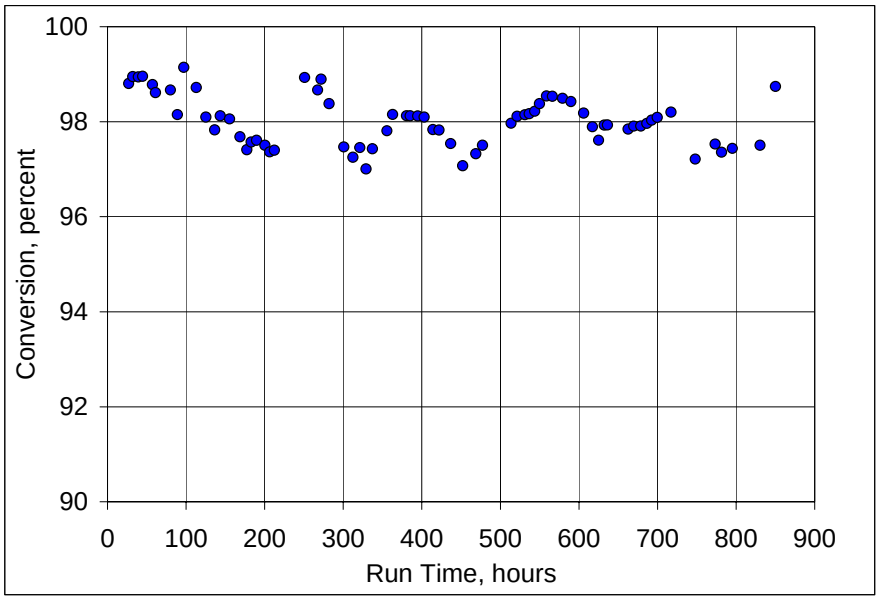

Figure 3-10. Carbon Conversion.

Gasification Efficiencies. Gasification efficiency is defined as the percentage of the energy fed that is converted to useful energy in the syngas. The two types of gasification efficiencies are cold gasification efficiency and hot gasification efficiency. The cold gasification efficiency is the percentage of energy fed that is available to a gas turbine as syngas latent heat. The hot gasification efficiency is the percentage of total energy fed that is available to produce electricity, which is the syngas latent heat recovered in a gas turbine plus the sensible heat recovered in a heat recovery steam generator. The hot gasification efficiency is the latent and the sensible heat of the syngas exiting the gasifier divided by the total amount of energy entering the gasifier, including the latent heat of the coal and the sensible heats of the air and steam. The efficiency boundary for the gasification efficiency values is the gasifier itself, not including downstream equipment.

During the air-blown operating periods, the cold gasification efficiencies ranged from 45.7 to 66.3 percent with an average of 62.3 percent. The cold gasification efficiency reached 67.7 percent during oxygen-blown operation. The hot gasification efficiencies were between 83.5 and 91.1 percent and averaged 90.0 percent for air-blown operations, and during oxygen-blown operation, the maximum value was 89.9 percent. An increase in gasification efficiency was realized as a result of the gasifier modifications, and is discussed in Section 3.5.

The two main sources of efficiency losses are the gasifier heat loss and the latent heat of the PCD solids. The estimated gasifier heat loss of 3.5 MMBtu/hr was about 12 percent of the feed energy, while the total energy of the PCD solids was 3 to 20 percent of the feed energy with the higher values occurring during periods of lower coal feed rates. A commercial Transport Gasifier will be more efficient than the PSDF gasifier due to the relatively lower nitrogen feed rate and the lower heat loss as a percentage of energy fed. The total enthalpy of the PCD solids can be decreased by decreasing both the PCD solids carbon content (i.e., heating value) and the PCD solids loading.

3.5 Gasifier Performance, Parametric Testing

A variety of tests were performed to characterize operation of the modified gasifier. Some of the parametric testing completed assessed coal feed rate effect on syngas heating value; temperature effect on carbon conversion, air distribution effect on temperature profile; and standpipe level effect on solids circulation rate.

Figure 3-11 plots the raw wet syngas heating value as a function of coal feed rate. This plot included steady state data taken in air-blown gasification mode. As seen in the figure, a positive correlation exists between the syngas heating value and coal feed rate. The higher coal rates produced higher syngas LHVs because the testing is done at relatively constant nitrogen feed rates, so the syngas concentration of nitrogen is lower at higher coal feed rates. The five data points from steady state operating periods TC20-5 through TC20-9 were offset below the main trend line, but still showed linear agreement. During these five operating periods, both coal feeders were operating and using nitrogen for conveying gas. This resulted in a higher nitrogen-to-coal ratio compared to using only one feeder. The additional nitrogen diluent caused the reduction in syngas heating value.

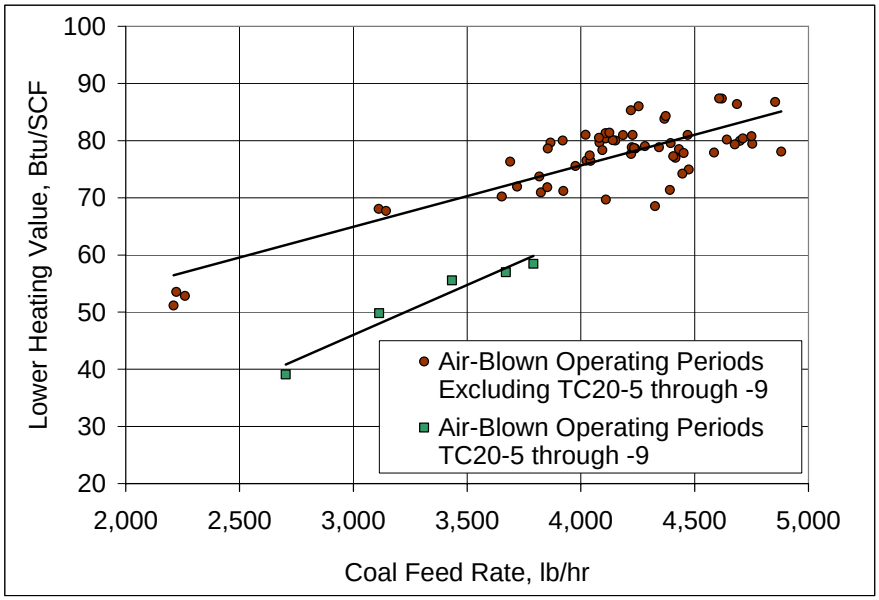

Figure 3-11. Syngas Lower Heating Value as a Function of Coal Feed Rate.

The coal feed rate is the variable that most directly affects gasification efficiency because of its impact on syngas heating value and thus on the syngas energy content. Figure 3-12 plots the air-blown cold gasification efficiency as a function of coal feed rate for TC18, TC19, and TC20, assuming 3.5 MMBtu/hr heat loss from the gasifier. The trends show a general increase in gasification efficiency for given coal feed rates after the TC20 gasifier modifications.

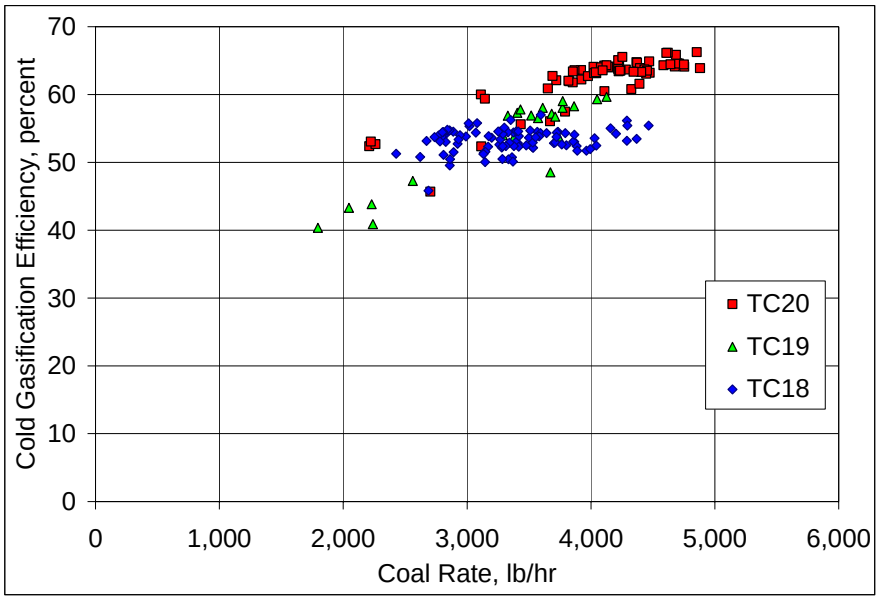

Figure 3-12. Comparison of Gasification Efficiencies versus Coal Rate for TC18, 19, and 20.

Figure 3-13 shows the effect of temperature on carbon conversion for the steady state operating periods. The plot shows the expected trend of increasing carbon conversion with increasing temperature, although the data is quite scattered due to the small range of temperatures tested. The modifications to the gasifier appear to have made near complete carbon conversion of PRB possible with limited sensitivity to temperatures in the range tested. Future testing of a wider range of temperatures may further quantify the impact of temperature on carbon conversion.

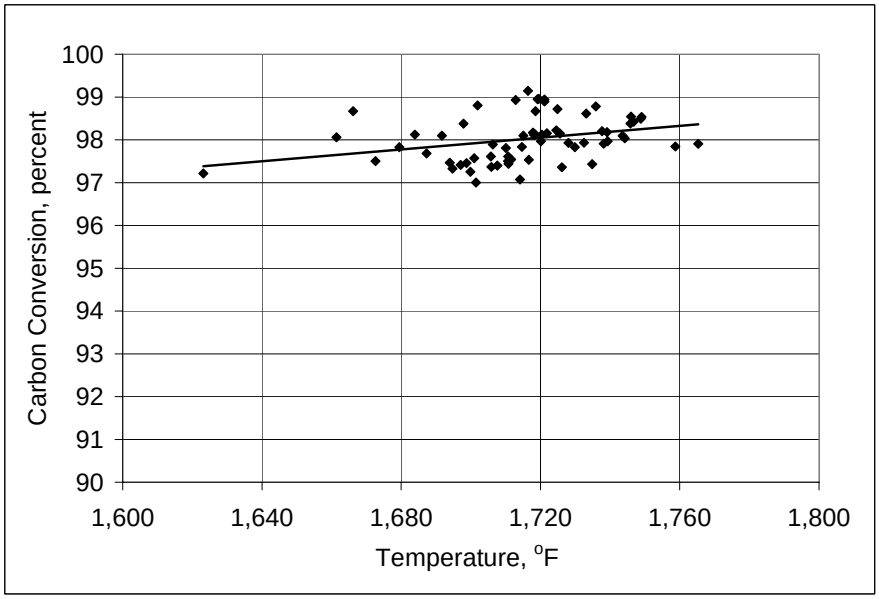

Figure 3-13 Carbon Conversion as a Function of Gasifier Temperature.

Another area of parametric testing assessed the effect of varying the air flow rate to the lower mixing zone (LMZ), specifically examining the effect of LMZ air flow rate on the gasifier temperature profile. For this analysis, data were taken when the standpipe level was maintained at 260 to 280 inH_2O, gasifier pressure was constant at 210 psig, and the coal feed rate was constant at approximately 3,600 lb/hr. Figure 3-14 shows the gasifier temperature differential between the maximum gasifier temperature and the LMZ temperature as a function of air flow rate to the LMZ (as a percentage of total air flow to the gasifier). As the air flow to the LMZ increased, less carbon was available for combustion in the LMZ. The temperature drop in the LMZ resulted in a larger temperature differential between the maximum gasifier temperature and the LMZ temperature.

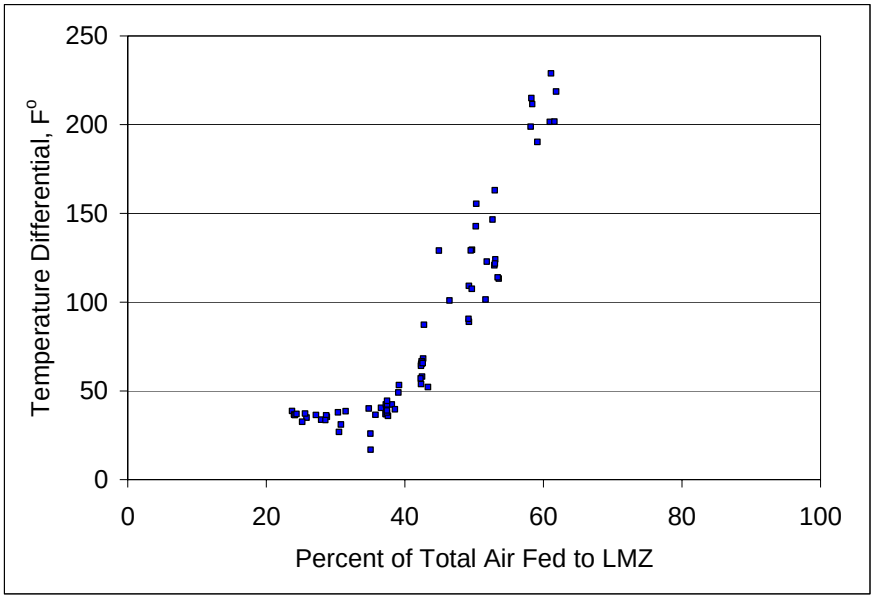

Figure 3-14. Gasifier Temperature Differential as a Function of Percent Air Fed to Lower Mixing Zone.

Figure 3-15 illustrates the relative solids circulation rate as a function of gasifier standpipe level (as measured by differential pressure). The data plotted are from all of the steady state periods. The standpipe level can be controlled within a very narrow range, but it was varied from about 120 to 300 inH_2O to evaluate the new gasifier design. As shown in the figure, the solids circulation rate showed a fairly linear relationship with the standpipe level.

Several other parameters were investigated to evaluate gasifier operation. Variations within the limits of stable operation in riser velocity, pressure, and circulation rate had little impact on gasifier operation. The effects of these three parameters on gasifier operation were thoroughly investigated, but no clear trends emerged from the effort.

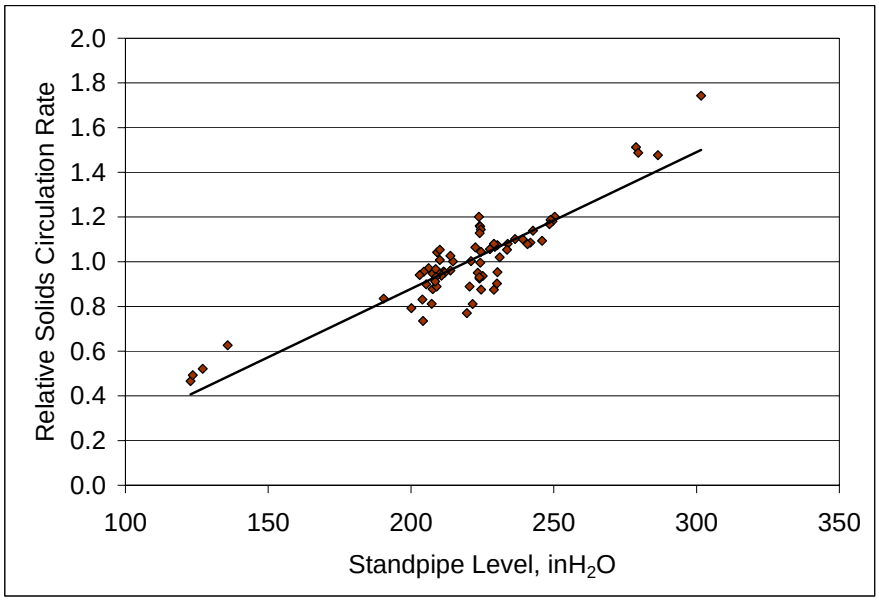

Figure 3-15. Circulation Rate as a Function of Standpipe Level.

3.6 Ammonia Injection Testing

A large portion of the coal-bound nitrogen is converted to ammonia in the gasifier, and in a commercial power plant based on Transport Gasifier technology, the ammonia would be recovered prior to syngas combustion in a gas turbine. Although the ammonia by-product would have significant economic value, under some circumstances it could be desirable to have the option of recycling the ammonia back to the gasifier for consumption. To understand the fate of additional ammonia injected into the gasifier, ammonia injection testing was performed during TC20.

Anhydrous ammonia was injected into the gasifier lower mixing zone on three separate occasions during TC20 to assess the effect on gasifier outlet ammonia concentrations. The test durations and the amounts and rates of ammonia injected are given in Table 3-5. Bottled ammonia with a purity of 99.99 percent was injected at rates one to three times the expected rate of ammonia generated during normal operation (with a coal feed rate of nominally 4,000 lb/hr).

Table 3-5. Ammonia Injection Tests.

Test Number	Test Date	Duration, min	Amount of NH_3 Injected, lb	Average Injection Rate, lb/hr
1	September 2, 2006	180	120	30 / 50 / 80
2	September 10, 2006	175	120	35
3	September 10, 2006	54	80	90

The gasifier outlet syngas ammonia concentration was monitored using an FTIR analyzer, and the nitrogen oxides (NOx) measurement from the continuous sampling system at the atmospheric syngas combustor outlet was monitored as well. Since the FTIR instrument can not be operated

continuously due to frequent buildup of condensable material, it was operated prior to each injection test for a period long enough to establish a baseline value of syngas ammonia concentration. Figure 3-16 gives the ammonia and NOx indications for the third test, which were typical of all three tests. The baseline level of NH_3 was typically around 2,500 ppm. NOx indications ranged from approximately 200 to 325 ppm. There was not a significant increase in either NH_3 or NOx when injections were performed. No change in syngas composition or heating value was discernable, since the flow rate of injected ammonia was low relative to the flow rate of major syngas constituents.

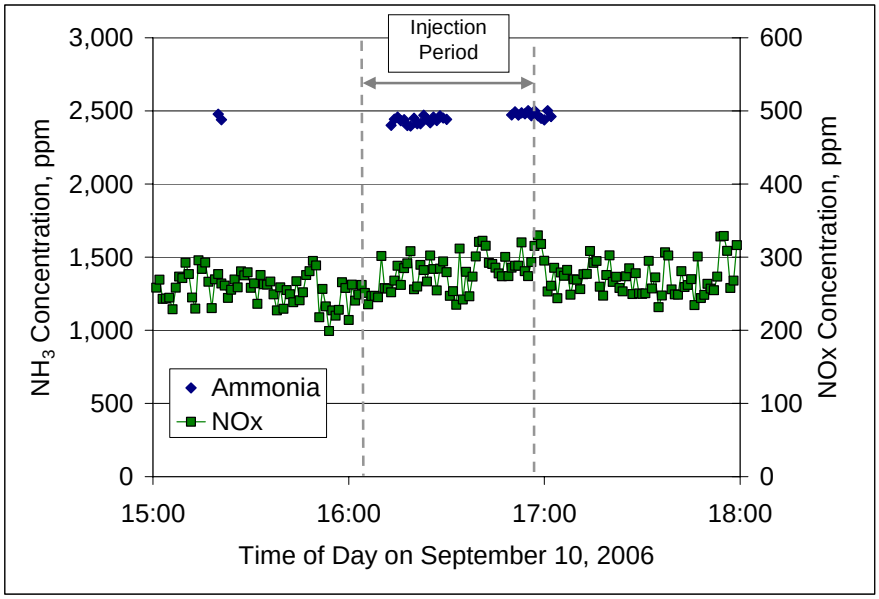

Figure 3-16. Ammonia and NOx Measurements during Ammonia Injection Testing.

3.7 Post-Test Campaign Inspections

Gasifier inspections were conducted from October 2 through October 9, 2006. After approximately 1,071 hours of solids circulation, including 870 hours on coal, all the refractory was in good condition.

The lower and upper mixing zone were inspected, and the walls were relatively clean. The lower mixing zone was inspected via the nozzle that is used to remove remaining solids after each test campaign. There was no agglomeration on the walls, and all of the aeration nozzles were clearly visible. The upper portion of the mixing zone was inspected via the nozzle where coal from the original feeder enters the gasifier. A small agglomeration had formed inside of the nozzle at the entrance to the mixing zone. The material did not protrude into the gasifier, and it was removed during the inspection. Also, a minimal amount of very fine, loose material had collected on the walls of the lower mixing zone and was easily removed.

A riser inspection was performed using a borescope from a nozzle at the top of the riser. The walls were clean and the refractory showed no wear. Both the primary and secondary crossovers

were also in good condition, with minimal refractory cracking. Some material remained in the secondary crossover.

The first solids collection device appeared to be in good condition. At the left of Figure 3-17 is a hairline crack seen from the entrance of the inspection nozzle that was approximately 1.5 inches deep. There was also a small area at the inlet with missing refractory, as shown on the right side of Figure 3-17.

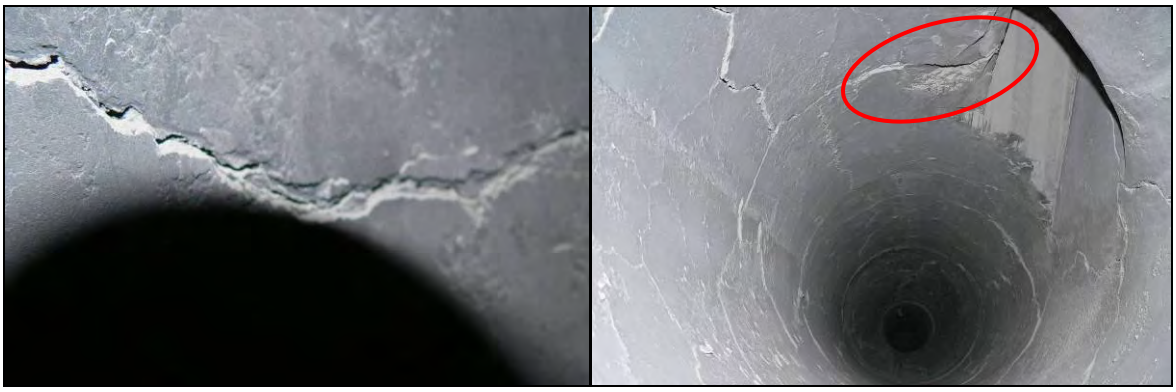

Figure 3-17. Inspection of the First Solids Separation Device.

The second stage of the solids collection device was in excellent condition. The inlet was smooth, and the hex mesh at the top was clearly visible.

The solids remaining in the seal leg were removed prior to the inspection. Visual inspection revealed that seal leg was also in good condition with no evident deposition.

A borescope inspection showed no deposits on the walls of the standpipe. A small amount of material remained in the bottom of the standpipe.

Inspection of the start-up burner leg showed that the walls were clean, and the inlet to the CCAD system did not have a significant amount of material.

Both the primary and the secondary gas cooler were visually inspected. Some of the tubes in the primary gas cooler were plugged, as shown in Figure 3-18, and these were cleared of material in preparation for the next test campaign. The tubes of the secondary gas cooler were clear, and a small amount of condensed organic material was present at the outlet.

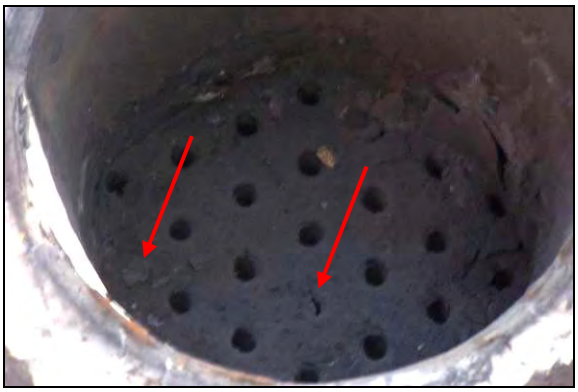

Figure 3-18. Inspection of the Primary Gas Cooler.

Photographs from the inspection of the atmospheric syngas combustor are presented in Figure 3-19. A patch of protruding refractory that was repaired below the sight glass after TC19 remained intact and was in good condition, as shown at the left of the figure. The middle photograph shows a portion of the vessel roof where a five inch thick portion of refractory around the downward pointing quench air nozzles had dislodged. The right-most photograph shows a damaged joint located between the outlet of the syngas combustor and the inlet of the heat recovery boiler. This joint had caused an internal hot spot during operation, and was repaired during the outage.

Figure 3-19. Inspection of the Atmospheric Syngas Combustor.

4.0 SENSOR DEVELOPMENT

4.1 Real-Time Particle Monitors

Although the in-situ measurements used to evaluate PCD outlet particulate concentrations at the PSDF give the most accurate results possible, commercial facilities will not be able to conduct such expensive and time consuming measurements daily. It is useful to have real-time, automated instruments to indicate the level of PCD collection performance and particulate penetration. Two real-time particulate monitors, the PCME DustAlert-90 and the Process Particle Counter (PPC) by Process Metrix, were evaluated in TC20.

4.1.1 PCME Dust-Alert-90

The DustAlert-90 particulate monitor from PCME, Ltd. is an electrodynamic instrument that senses naturally occurring charge on particles flowing past a simple rod-like probe inserted into the syngas stream. The monitor, referred to as the PCME, was operational throughout TC20, although the data it collected were generally unremarkable since particulate loadings were low throughout most of the test campaign. The PCME was not able to detect the elevated loadings at the start of the test campaign (discussed in detail in Section 5 and Table 5-1). Even the 2.35 ppmw measured in combustion mode during start-up was not clearly detected. The backpulse spikes on the PCME output trace were elevated during this start-up period (the first indication of increased loading) but there was no clear increase in the baseline trace. Since it has been shown in the past that this instrument is not sensitive to small particles, it appears that the size distribution at this time was probably too fine for the PCME to detect.

Particulate injection into the PCD outlet piping was conducted late in the test campaign using a fluidized-bed particulate injection system designed and built expressly for this purpose. The injection period corresponded to in-situ Outlet Run Number 30 from Table 5-1, where an actual particulate concentration of 8.4 ppmw was measured. The real-time response and five minute average of the PCME is displayed in Figure 4-1. The PCME gave a clear response to the beginning and end of the particulate injection and returned an average value of 4.9 percent over the period that comparative measurements were made. Figure 4-2 gives the TC20 result for actual particulate concentration versus PCME output compared to previous tests. Since the PCME measures particles per unit time rather than concentration, the results in the figure have been normalized to a syngas flow of 25,000 lb/hr. The normalized TC20 result (5.1 ppmw) falls above the linear regression line to all previous data.

4.1.2 Process Metrix Process Particle Counter

The PPC particulate monitor is a sampling system consisting of a sample extraction system designed by Southern Research Institute (SRI) and Gas Technology Institute (GTI) and a light scattering optical particle counter designed by Process Metrix, LLC.

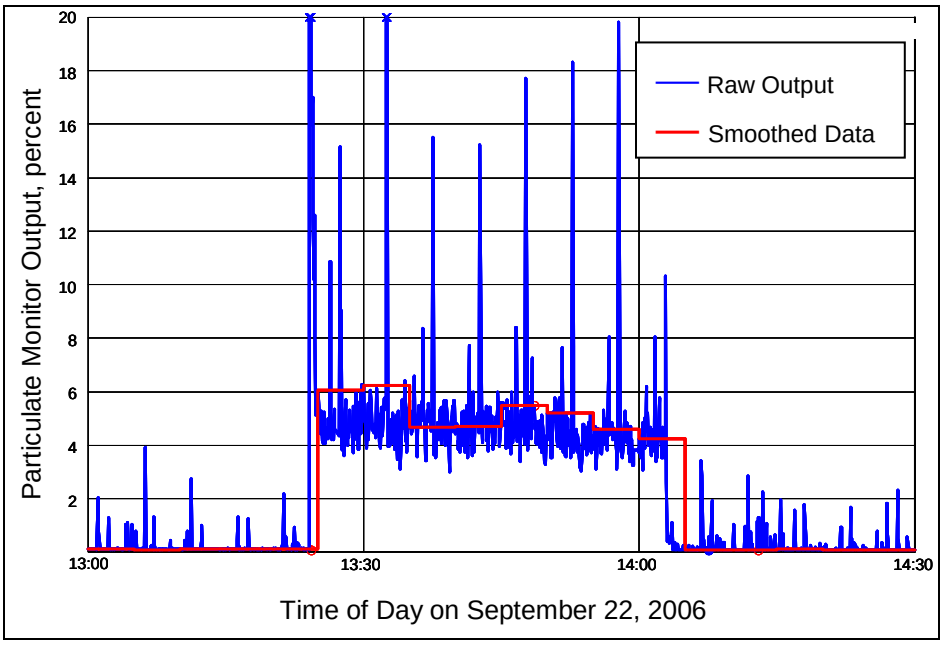

Figure 4-1. PCME Particulate Monitor Response to Particulate Injection.

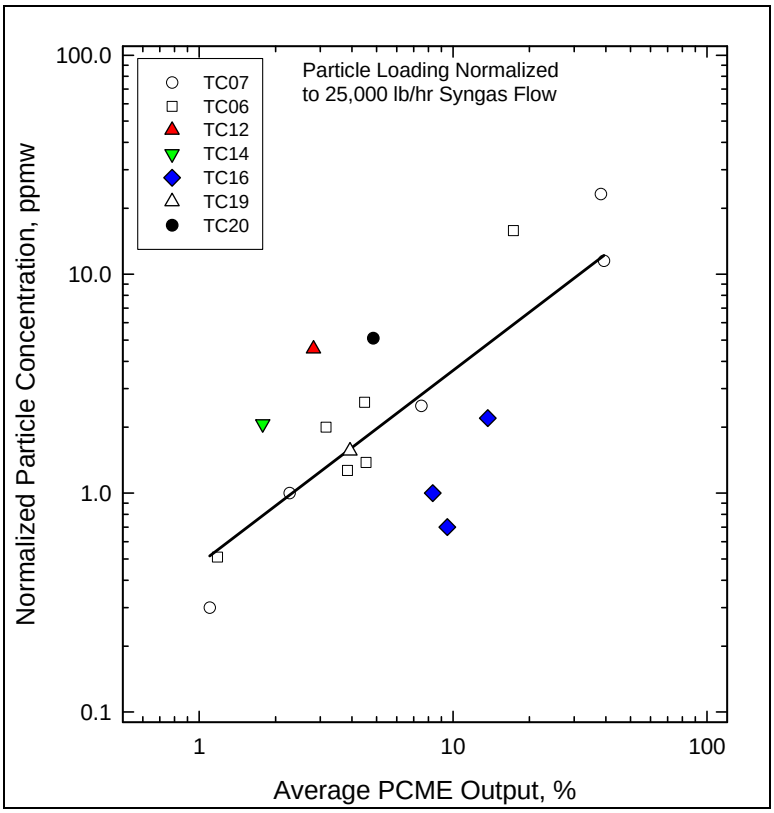

Figure 4-2. PCME Particulate Monitor Response to Particulate Injection for Several Test Campaigns.

During TC19, the PPC had problems with condensation of water and organic components of the syngas fouling the windows of the optical cell. During the outage prior to TC20, Process Metrix redesigned the cooling water passages in the optical head to limit cooling of the syngas while still protecting the windows. Heaters for the cooling water and for the nitrogen window purge were also designed and procured, but construction schedule limitations prevented the installation of the heaters prior to TC20. However, since no permanent damage would result from operating the instrument too cool, data collection was attempted during TC20 without all of the modifications.

Changing the cooling water passages may have slightly improved window contamination, but disassembly of the instrument was required every few days to clean the windows. Even when the windows were clean, the PPC output was erratic for most of TC20 with periods of very low particle counts (consistent with actual particle concentrations) mixed with periods where the PPC indicated particle concentrations of thousands of ppmw that clearly were incorrect. It was eventually discovered that sample gas flow through the optical cell affected the measured concentration. Figure 4-3 shows the output of the PPC in the upper pane and the flow rate through the optical cell in the bottom. Repeated experimentation indicated that operation at 40 lb/hr of syngas flow produced stable particle readings and was sufficient gas flow to keep the system reasonably warm. Flows much higher than 40 lb/hr caused increasing particle counts. The cause of this phenomenon is unknown, but it is possible that the higher flow rates produced more turbulence at the optical cell entrance, resulting in more rapid entrainment of the cool nitrogen purge gas and increased condensation of organic material and water vapor.

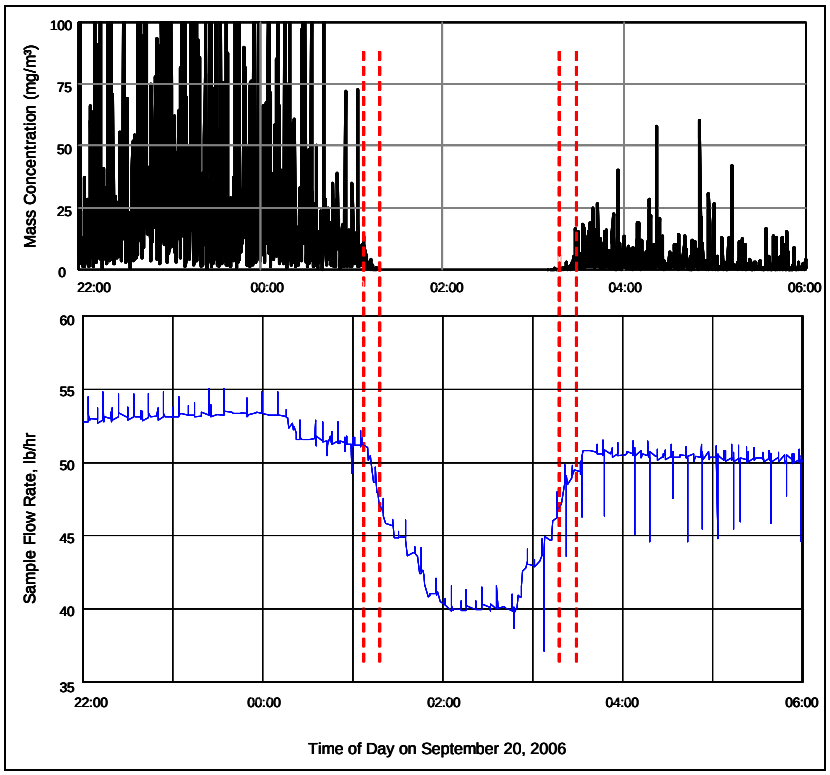

Figure 4-3. Changes in PPC Particulate Monitor Output with Sample Flow Rate.

During the particulate injection test discussed previously, the PPC produced the output displayed in Figure 4-4. The instrument was operated at 30 lb/hr flow with clean windows. The instrument clearly indicated a negligible background concentration before and after injection with sharp increase to an average value of 2.7 ppmw during injection. While the PPC value is a little less than half of the actual particulate concentration, the agreement was considered reasonable at this stage of instrument development. More PPC data will be collected in the future after the heaters have been installed on the coolant and window purge lines.

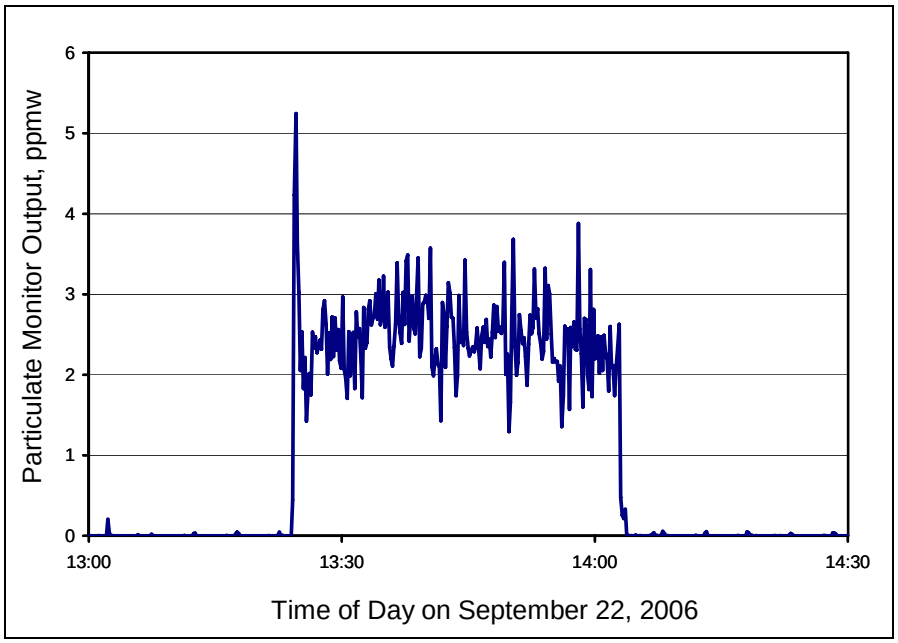

Figure 4-4. PPC Particulate Monitor Response to Particulate Injection.

4.2 Pressure Differential Indicator Ceramic Inserts

To reduce instrument purge flow requirements and reduce plugging problems, ceramic inserts were installed on three gasifier pressure differential indicators (PDIs). These porous, ceramic inserts, manufactured by Foreman Instrumentation and Controls, prevent solids flow into the instrument, thereby reducing the amount of required purge flow by over 50 percent.

Ceramic inserts were installed on two PDIs on the riser and one PDI on the seal leg. The ceramic inserts on the riser are the SGC05 design, a high differential pressure, low purge flow design. The seal leg differential pressure was fitted with MAC10 inserts, a low differential pressure, higher purge flow design. The SGC05 design has lower purge flow requirements but may be more prone to plugging. The main objective for insert testing during TC20 was to evaluate operability.

Measurements with the ceramic tipped purge ports compared well with the standard measurements, as indicated in Figure 4-5. The two SGC05 designs compared well to standard

PDI measurements in similar locations. The MAC10 data in Figure 4-5 did not compare as well to the standard measurement since the purge ports were located at slightly different elevations on the seal leg. Although the distance between the ports was the same, the test ports were approximately one foot lower than the standard measurement. Variability in the density in this region caused a difference in calculations. However, the test PDI showed promise since the ports did not plug in this area of high solids concentrations.

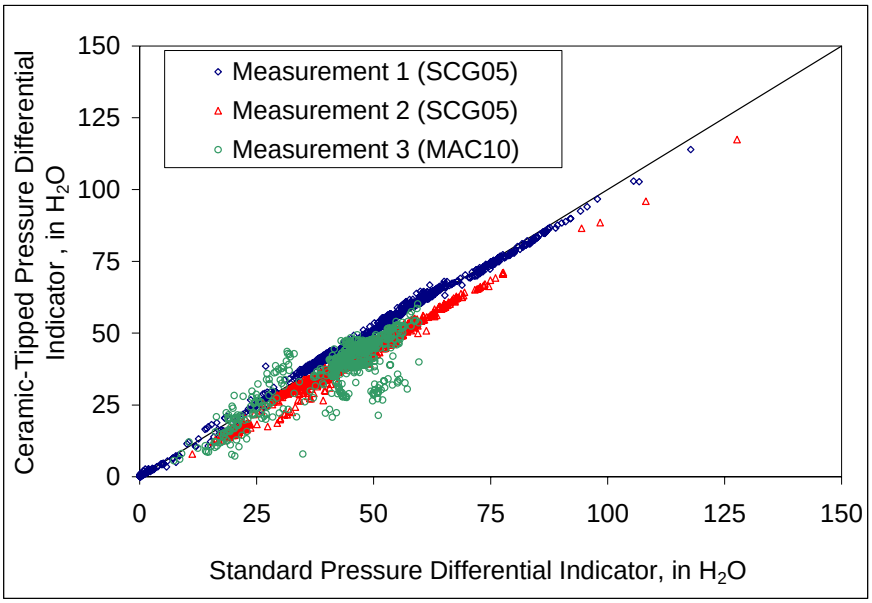

Figure 4-5. Measurements of Ceramic-Tipped Pressure Differential Indicators Compared to Standard Pressure Differential Indicators.

4.3 Thermowell Inserts

Thermowell durability is a primary concern for reliable temperature measurements in the gasifier due to erosive and corrosive operating conditions. In addition, thermowell materials must handle rapid temperature changes. During TC20, two types of thermowell materials, metal (HR-160) and ceramic, were tested. There were no failed gasifier temperature measurements during the test campaign. This was a significant improvement from past test campaigns during which multiple measurement failures typically occur. In TC19, seven temperature measurements failed while in TC18, 12 measurements failed. The improvement in TC20 may have been partially attributable to the lower operating velocity in the gasifier, a result of the gasifier modifications discussed previously.

5.0 PARTICULATE CONTROL DEVICE

A major goal of TC20 was to evaluate the effect of the gasifier modifications on PCD performance, since these modifications were expected to decrease the size distribution and the concentration of the particulate carried over to the PCD. Secondary goals included evaluation of the collection efficiency of HR-160 filter elements and evaluation of a new failsafe media configuration.

The effects of the gasifier modifications on the PCD particulate characteristics and the collection performance were quantified by in-situ particulate sampling at the inlet and outlet of the PCD and by physical and chemical analyses. Further analyses of failsafe performance, pressure drop performance, and filter element condition were completed.

Development and validation of real-time particle monitors for evaluating PCD outlet particulate concentration has previously been reported in this section on PCD performance. However, starting with the TC20 report, this work is described in Section 4.0, Sensor Development. Where appropriate, the performance of the monitors will be compared to results presented in Section 5.2.

5.1 PCD Particulate Collection Performance

In-situ particulate sampling was performed at the PCD inlet and outlet using the in-situ batch sampling systems described in previous reports. The inlet particulate measurements were used to help understand the pressure drop characteristics of the PCD and were used to calculate the transient drag of the particulate in a later section of this report. The outlet measurements indicated the collection performance of the PCD with the installed filter elements. This section will also discuss failsafe tests conducted during TC20.

5.1.1 PCD Inlet Mass Loadings

Particle mass concentrations and mass rates measured at the PCD inlet are given in Table 5-1. To assess the performance of modified gasifier, the first eight samples at the PCD inlet were taken during sand circulation with no coal feed. As expected with the high efficiency of the gasifier solids collection, carryover to the PCD was very low, generally less than 10 lb/hr.

During air-blown gasifier operation, an additional 24 samples were collected, and one sample was collected during oxygen-blown gasification. The modified gasifier solids separation unit was more efficient than the previous configuration. The average inlet mass rate for all of TC20 was 173 lb/hr (7800 ppmw) compared to 282 lb/hr (1270 ppmw) for TC19. The solids mass rates are plotted as a function of coal feed rate in Figure 5-1. This graph indicates that the solids mass carried over to the PCD was lower for all coal feed rates during TC20. The solid line is a linear regression to the TC20 data, while the dashed lines are for selected past test campaigns. The reduced particulate flow to the PCD would tend to lower pressure drop. However, other potential changes (e.g., finer particle size and higher drag) could increase pressure drop. These other effects are discussed later.

Table 5-1. In-Situ Particulate Measurements.

	PCD Inlet					PCD Outlet				
Test Date	Run No.	Start Time	End Time	Particle Loading, ppmw	Particle Loading, lb/hr	Run No.	Start Time	End Time	H_2O Vapor, vol %	Particle Loading, ppmw
Sand Circulation										
8/2/06	1	10:33	10:53	65	0.83	1	9:30	13:30	1.4	0.56
	2	15:41	16:41	172	3.55	--	--	--	--	--
8/3/06	3	8:52	9:07	1755	27.7	2	9:30	13:30	2.9	0.58
	4	12:30	12:30	412	6.45	--	--	--	--	--
8/6/06	5	7:30	8:30	241	2.88	--	--	--	--	--
	6	10:30	11:30	436	7.62	--	--	--	--	--
8/7/06	7	10:57	11:57	486	8.72	3	9:45	1:45	2.8	0.19
	8	14:30	15:30	325	5.89	--	--	--	--	--
PRB Combustion										
8/8/06	--	--	--	--		4	16:00	16:20	14.5	2.35
PRB Gasification - Air Blown										
8/9/06	9	13:30	13:45	7400	172	5	12:45	14:30	6.7	0.43
8/10/06	10	9:41	10:11	4510	105	6	9:00	13:00	6.8	0.34
8/11/06	11	12:30	13:00	4935	102	7	10:35	14:35	8.7	0.23
8/12/06	12	9:00	10:00	5520	119	8	8:30	12:30	7.4	0.22
8/14/06	13	9:00	9:20	6659	164	9	8:45	12:29	6.2	0.13
8/15/06	14	8:30	9:00	5483	139	10	8:15	12:15	10.4	0.13
8/16/06	15	9:15	9:30	7992	203	11	8:30	12:30	8.3	(1)
8/17/06	16	10:05	10:18	7682	186	12	8:30	12:30	6.9	0.17
8/29/06	17	12:30	12:45	6044	102	13	10:15	14:15	8.1	< 0.10
8/30/06	18	9:00	9:15	5408	92	14	8:45	12:45	9.7	0.11
8/31/06	19	9:00	9:15	7970	155	15	8:30	12:30	8.9	0.10
9/1/06	20	9:30	9:45	9645	224	16	10:07	11:07	7.4	0.45 (2)
9/4/06	21	9:00	9:15	7743	171	17	8:30	12:30	8.6	0.12
9/5/06	22	9:00	9:15	8538	187	18	8:30	12:30	9.6	0.07
9/6/06	23	12:15	12:25	10955	254	19	12:00	13:00	9.1	0.30 (2)
9/7/06	24	12:15	12:30	10099	232	20	8:30	12:30	9.5	< 0.10
9/8/06	25	9:05	9:20	8725	195	21	8:30	12:18	9.0	< 0.10
9/11/06	26	9:35	9:50	6729	144	22	9:15	11:20	9.1	< 0.10
9/12/06	27	9:00	9:15	6168	141	23	8:30	12:30	8.3	< 0.10
9/13/06	28	12:45	13:00	6151	139	24	12:00	14:00	7.3 (3)	0.12
9/14/06	29	9:00	9:15	8402	219	25	8:30	12:30	10.5	< 0.10
9/18/06	30	9:00	9:15	7155	165	26	8:30	12:30	6.9 (3)	(4)
9/19/06	31	9:10	9:25	10659	243	27	9:00	10:14	10.9	< 0.10
9/20/06	32	12:35	12:50	9919	226	28	9:30	13:30	6.2	< 0.10
9/21/06	33	10:30	10:45	9491	223	29	8:45	12:45	7.0	< 0.10
PRB Gasification - Oxygen Blown										
9/22/06	--	--	--	--	--	30	13:30	14:00	28.4	8.4 (5)
9/23/06	34	9:05	9:20	11864	186	31	9:00	10:00	18.0	< 0.10

Notes:
1. Value not reported. Probable weighing error.
2. Pall failsafe leak test - Not a PCD leak.
3. Steam addition changed during test.
4. Coal feeder trip. Sample contaminated.
5. Dust injection for particle monitor calibration. Not a PCD leak.

* - Normalized dustcake drag in units of inwc/(ft/min)/(lb/ft^2)

The gasifier solids collection efficiency appeared to change time during TC20. The average mass loading to the PCD during the first half of the test campaign (Runs 9 to 18) was 6,200 ppmw, while the average for Runs 19 to 33 was 8600 ppmw. This change may be due to a "breaking-in" period for the cyclones or other effects, but the same effect was seen in particle size and drag, as discussed in later sections.

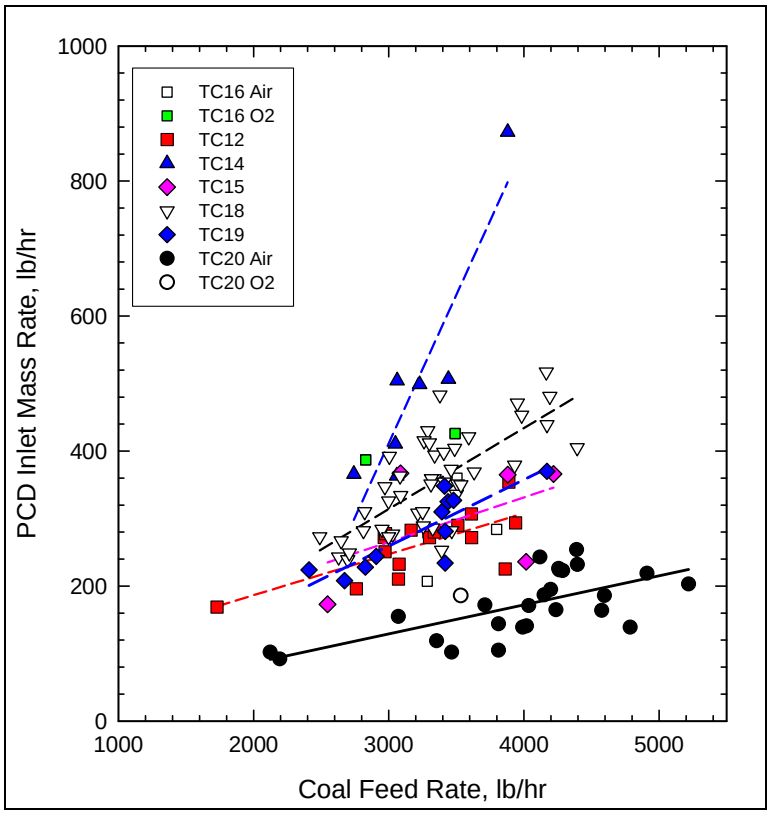

Figure 5-1. PCD Inlet Particulate Concentration as a Function of Coal Feed Rate.

5.1.2 PCD Outlet Mass Loadings

Particle concentrations measured at the PCD outlet are included in Table 5-1 and are plotted as a function of time in Figure 5-2. For comparison, the graph also contains values measured during TC18 and TC19. Bars in the graph that are below the "Minimum Measurement Resolution" line are not actually measured values but are merely placeholders to indicate the numbers of samples that had immeasurably low concentrations. The data plotted for TC20 do not include the results for the long period of sand circulation but start with coal feed to the gasifier.

As discussed in previous reports, it is common to see an elevated particulate concentration at the outlet of the PCD during the first few days of a test campaign. This may be due to seasoning of filter elements and plugging of gasket pores or to particulate from corrosion products and mechanical assembly of the PCD. At the start of TC20 the particulate loadings remained above 0.1 ppmw (the minimum measurement resolution) continuously for 10 days of operation, which is about twice as long as usual. Also, even after the first test that was below measurement resolution, values tended to increase back above 0.1 ppmw through Day 25 of TC20.

At the time, the elevated loadings and variation in performance appeared to be caused by the lower collection efficiency of the Dynalloy filter elements. Cold flow model tests indicated that a new Dynalloy sintered metal fiber filter had about 50 times the penetration rate of a new iron aluminide sintered metal powder filter. After seasoning for 400 hours in the PCD, the cold flow model penetration rate of the Dynalloy filter was down to about 1.6 times the penetration rate of the iron aluminide filter. Although there is no data on Dynalloy seasoning rate prior to TC20, the elevated loadings and increased seasoning time seemed reasonable when compared to previous experience with the iron aluminide elements.

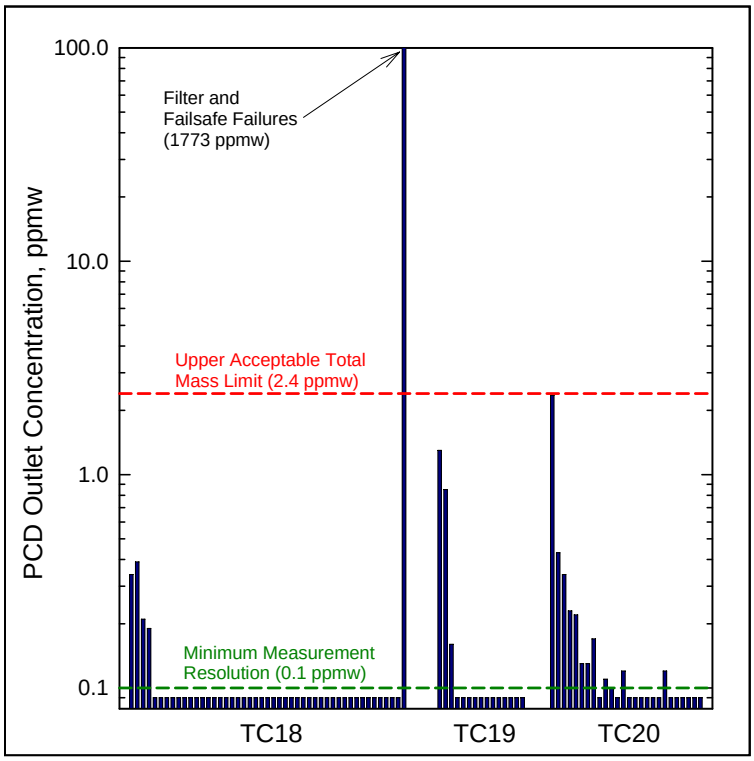

Figure 5-2. PCD Outlet Particulate Concentrations for Recent Gasification Test Campaigns.

Some fraction of the black particulate (thought to be gasification ash) collected on the outlet sample filters appears to be corrosion product from the outlet side of the PCD. This complicated the analysis of PCD performance somewhat, but the results for TC20 are largely correct and provide a reasonable indication of the performance of the Dynalloy filter elements. Unfortunately, there is no technique to distinguish between the mass of corrosion product and gasification ash penetrating the PCD, and the ultimate accuracy of the results is uncertain.

Regardless of the corrosion issues that may increase measured particulate penetration rates, the collection efficiency of the Dynalloy filter elements was at least high enough to keep the outlet particulate concentrations adequately low. The main conclusion relative to the Dynalloy filter elements is that they are not as efficient as the iron aluminide elements, but they appear to provide acceptable collection performance with less evidence of corrosion.

5.1.3 Failsafe Performance Tests

During TC20 the new valve-activated failsafe tester described in the TC19 report was used to simulate a catastrophic filter element failure and determine the effectiveness of a new type of failsafe. The failsafe tested during TC20 was a Pall prototype metal fiber fuse in HR-160 alloy. The fuse is similar to a Dynalloy HR-160 filter element except that the media is reversed to encourage the failsafe to plug instead of acting as a surface filter when it is exposed to elevated particulate loading. Normal Dynalloy filter elements have a layer of fine fibers on the outside surface with coarser underlying support fibers. The failsafe that was tested in TC20 had the finer fibers on the inside surface so that particles will tend to penetrate down into the coarse fibers, be collected in the mesh of finer fibers, and thus blind the failsafe to further gas flow.

The initial test of the prototype reverse Dynalloy failsafe was conducted as Outlet Run Number 16 on September 1, 2006. This measured the failsafe performance over the first hour of exposure to the simulated leak. A value of 0.45 ppmw was measured, which was clearly elevated but still within safe operating limits. The background concentration without injection was right at 0.10 ppmw. The failsafe tester was shut down at the end of the test on September 1, 2006. The failsafe test was restarted with Outlet Run 19 on September 6, 2006, where a value of 0.30 ppmw was measured for the first hour. This time the valve was left open and a second test performed on the next day during the period of 20.5 to 24.5 hours of exposure. This longer term test indicated that the particle concentration was below 0.10 ppmw.

The initial performance of the reverse Dynalloy failsafe was not quite as good as the Pall iron aluminide fuse tested in TC19. Although that test was assigned a value of less than 0.15 ppmw because of contamination of condensed material, microscopic inspection of the TC19 sampling filter indicated that initial particle leakage through the iron aluminide failsafe was probably less than 0.10 ppmw. While the iron aluminide fuse has good particle collection characteristics, experience has shown that it is prone to breakage in the heat-affected zone near the flange weld. While the particle collection characteristics of the Dynalloy failsafe are not quite as good as those of the iron aluminide fuse, the Dynalloy failsafe is more durable and may prove to be the best choice for use in a commercial plant.

5.1.4 Filter Element Sealing Issues

As discussed in the TC19 Report, the use of rolled-construction gaskets in combination with the conical washers eliminated the problems with torque loss on the filter element and failsafe bolts. Torque measurements confirmed this finding after TC20 as well. Evaluation of bolt torques will continue.

5.2 PCD Solids Analysis

Important characteristics of the PCD solids include particle size distribution, bulk density, true density, porosity, surface area, composition, and flow resistance. The effect of all these parameters must be considered when analyzing the performance of the PCD.

5.2.1 Particle Size Distributions

A Microtrac X-100 particle size analyzer was used to measure the particle size distributions of the in-situ particulate samples collected at the PCD inlet and the PCD hopper samples used for the lab drag measurements. The most significant change in particle parameters expected to result from the gasifier modifications completed prior to TC20 would be a shift in particle size distribution. Cyclones do not collect particles across all sizes, but tend to retain the largest particle fractions, leaving a higher percentage of small particles. A very fine size distribution can contribute to high PCD pressure drop.

In-Situ Samples. Figure 5-3 shows two average differential mass particle size distributions measured on the TC20 PCD inlet in-situ samples and compares these data to a similar distribution from TC19. Both of the TC20 distributions showed that a significant amount of mass between 20 and 40 microns was removed by the new cyclone system. However, comparison of the particle size data for the first half of TC20 and the second half of the test campaign suggested that the gasifier solids collection devices were becoming less efficient with time. Figure 5-4 plots the mass median diameters of the in-situ samples for the entire test campaign. Although there is considerable scatter in the data, the dashed regression line indicates an increase in MMD from under 6 microns at the start of TC20 to over 11 microns at the end. Particle size differences would be expected to have a noticeable effect on PCD pressure drop, which will be further discussed in a later Section 5.2.2.

Hopper Samples. Figure 5-5 compares the differential mass percentage distributions for the in-situ samples from the two halves of the test campaign with the hopper samples used for the TC20 lab drag measurements. (Although the in-situ samples are a more accurate representation of the particulate entering the PCD at a given time, the quantity of particulate collected is far too small to be useful for drag measurements.) The three hopper samples were chosen because they were collected during periods when the PCD pressure drop indicated high, moderate, and low drag particulate. The size distributions show differences related to the drag properties. The first half in-situ distribution includes an elevation at the small end of the distribution and the fewest large particles. These characteristics generally relate to high drag particulate. The low and moderate drag samples are more like the second half in-situ sample with increased numbers of large particles which should lower drag.

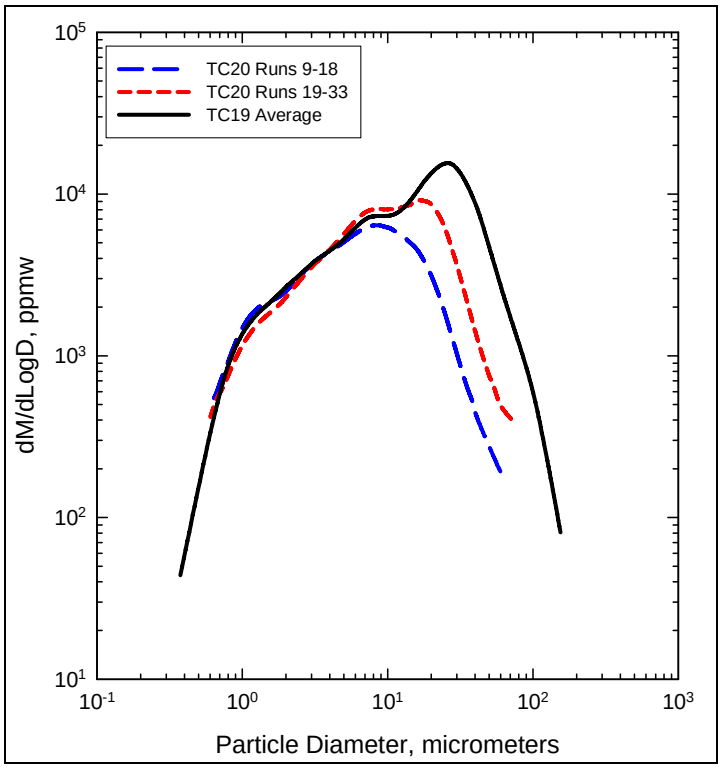

Figure 5-3. Comparison of Particle Size Distributions from In-Situ Samples.

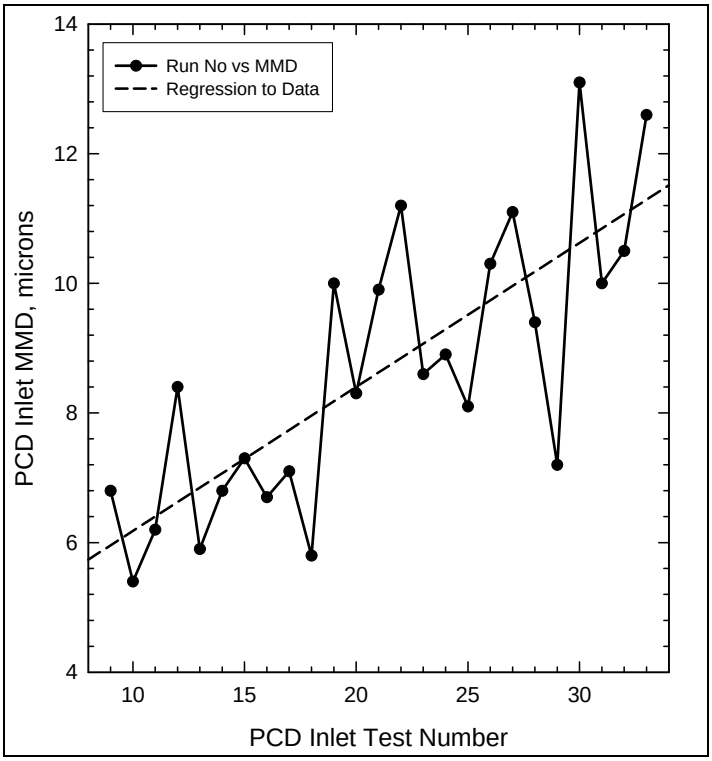

Figure 5-4. Change in Median Particle Diameter with Time.

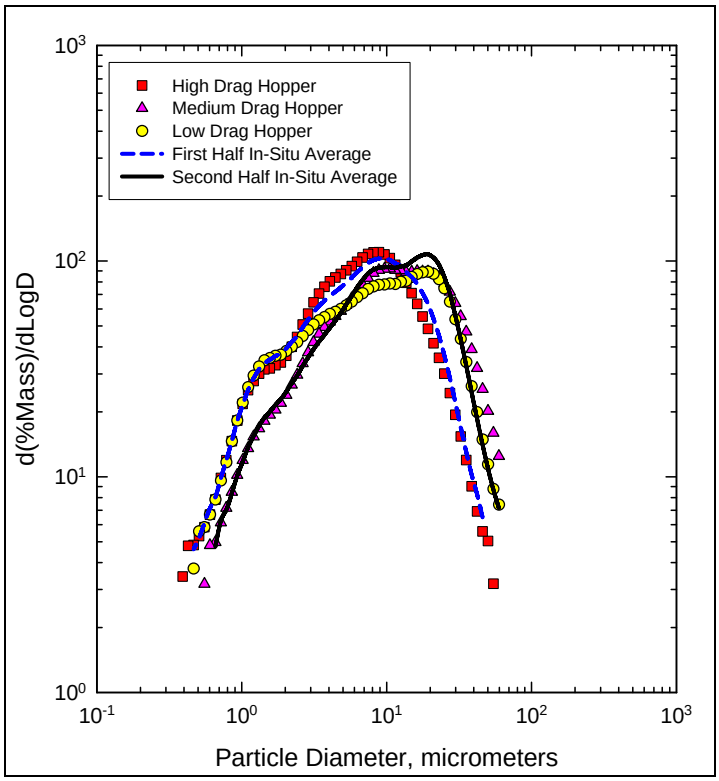

Figure 5-5. Comparison of Particle Size Distributions.

5.2.2 Dustcake Observations and Thickness and Areal Loading Measurements

Based on observations of the dustcake, the semi-dirty shutdown performed at the end of TC20 appeared to be successful, preserving the entire dustcake (transient plus residual) on the top plenum and only the residual dustcake on the bottom plenum. Measurements of dustcake thickness and areal loading are given in Table 5-2. As expected, the transient dustcake areal loading was lower than in previous test campaigns with PRB coal due to the lower solids carryover with the new gasifier configuration. Based on the average loading of transient dustcake (0.082 -0.022 = 0.060 lb/ft^2), the predicted PCD inlet solids rate would be:

$$\text{Inlet solids} = 0.060\ \text{lb/ft}^2 \times 256.18\ \text{ft}^2 / 5\ \text{min} \times 60\ \text{min/hr} = 184\ \text{lb/hr}.$$

This agrees well with the inlet solids rate measured on the last day of testing, which was 186 lb/hr. This comparison suggests that there was essentially no dropout of solids in the PCD vessel upstream of the filter elements.

It was expected that the transient dustcake areal loading was lower in TC20 than in previous test campaigns, although the lower residual dustcake areal loading observed was not anticipated. The low residual dustcake areal loading may partly explain the relatively low baseline pressure drop observed at the end of TC20.

Table 5-2. Dustcake Thickness and Areal Loading Measurements.

Element No.	Element Type	Failsafe Type	Dustcake	Thickness in.	Areal Loading lb/ft^2	Calculated Porosity %
Top Plenum						
T-3	FEAL	PSDF	Transient + Residual	0.0589	0.070	89.6
T-9	FEAL	PSDF	Transient + Residual	0.0695	0.085	89.3
T-17	HR-160	SW Down	Transient + Residual	0.0723	0.090	89.1
Average				*0.0669*	*0.082*	*89.3*
Bottom Plenum						
B-6	HR-160	PSDF	Residual Only	0.0140	0.021	87.1
B-9	HR-160	PSDF	Residual Only	0.0136	0.023	85.3
B-14	HR-160	PSDF	Residual Only	0.0138	0.022	86.2
Average				*0.0138*	*0.022*	*86.2*
Average Measurements from Previous PRB Runs						
Previous Dirty Shutdown Average			*Transient + Residual*	*0.070*	*0.147*	*81.4*
Previous Clean Shutdown Average			*Residual Only*	*0.016*	*0.041*	*77.6*

5.2.3 Particulate Physical Properties and Chemical Composition

Due to the large number of in-situ samples collected during TC20, measurements of the physical properties and chemical composition were performed on only a selected subset of samples, that were representative of stable operation. This section discusses the physical properties and chemical compositions of the selected in-situ samples collected at the PCD inlet, the PCD hopper samples used for the lab drag measurements, and the dustcake samples.

In-situ Samples. Tables 5-3 and 5-4 give the physical properties and chemical compositions of the in-situ samples collected at the PCD inlet and the hopper samples selected for lab drag measurements. All of the in-situ samples have fairly consistent physical properties and chemical compositions, except for Run Numbers 11 and 18, which have unusually low surface areas and carbon contents. In the past, it has been observed that surface area decreased with decreasing carbon content. This effect was seen again in TC20 as illustrated in Figure 5-6. As seen in the past, the change from air-blown operation to oxygen-blown operation did not have any effect on the particulate properties and chemical composition.

Hopper Samples. For lab drag measurements, three hopper samples were selected from periods of apparently high drag, medium drag, and low drag (based on PCD transient drag values determined from PCD pressure drop, gas flow, and solids loading). As shown in the tables mentioned above (5-3 and 5-4), the sample with the lowest carbon content also had the lowest

surface area. However, the samples with medium and high carbon content were reversed in surface area. All of the hopper samples appear to be very similar to the corresponding in-situ samples collected under the same test conditions. This suggests that the hopper samples selected are representative samples for the lab drag measurements.

Table 5-3. Physical Properties of In-Situ Samples and Samples Used for Lab Measurements.

Sample ID	Run No.	Sample Date	Bulk Density, g/cc	True Density, g/cc	Bulk Porosity, %	Surface Area, m^2/g	Mass Median Particle Size, µm	Loss on Ignition, %
In-Situ Samples, PRB, Air-Blown								
AB21127	11	08/11/06	0.33	2.71	87.8	63	6.2	11.13
AB21221	13	08/14/06	0.23	2.24	89.7	186	5.9	45.07
AB21223	15	08/16/06	0.24	2.39	90.0	163	7.3	37.38
AB21318	18	08/30/06	0.30	2.69	88.8	39	5.8	10.43
AB21539	20	09/01/06	0.21	2.38	91.2	191	8.3	37.65
AB21700	25	09/08/06	0.18	2.47	92.7	145	8.1	34.99
AB21702	27	09/12/06	0.20	2.64	92.4	155	11.1	23.90
AB21927	31	09/19/06	0.19	2.28	91.7	170	10.0	40.18
In-Situ Samples, PRB, Oxygen-Blown								
AB21930	34	09/23/06	0.22	2.45	91.0	162	10.8	31.44
Samples Used for Lab Drag Measurements								
AB22026	High Drag	8/14/06	0.21	2.30	90.9	159	6.1	39.03
AB22027	Low Drag	8/30/06	0.27	2.63	89.7	82	8.0	15.37
AB22028	Med Drag	9/20/06	0.21	2.42	91.3	181	9.8	31.08

Table 5-4. Chemical Composition of In-Situ Samples and Samples Used for Lab Measurements.

Sample ID	Run No.	Sample Date	$CaCO_3$ Wt %	CaS Wt %	CaO Wt %	Non-Carbonate Carbon Wt %	Inerts (Ash/Sand) Wt %	Loss on Ignition Wt %
In-Situ Samples - PRB Coal - Air-Blown								
AB21127	11	08/11/06	1.00	0.25	22.90	10.58	65.28	11.13
AB21221	13	08/14/06	2.25	3.11	10.89	43.75	39.99	45.07
AB21223	15	08/16/06	2.55	1.00	15.85	34.74	45.86	37.30
AB21318	18	08/30/06	0.59	0.29	23.10	9.40	66.62	10.43
AB21539	20	09/01/06	2.86	1.53	12.99	35.47	47.14	37.65
AB21700	25	09/08/06	2.93	1.03	16.93	33.09	46.02	34.99
AB21702	27	09/12/06	2.75	0.76	18.31	22.14	56.04	23.90
AB21927	31	09/19/06	3.36	0.27	16.49	36.98	42.91	40.16
In-Situ Samples - PRB Coal - Oxygen-Blown								
AB21930	34	09/23/06	2.52	0.40	18.99	29.40	48.68	31.44
Samples Used for Lab Drag Measurements								
AB22026	High Drag	08/14/06	3.09	2.14	16.17	37.74	40.86	39.03
AB22027	Low Drag	08/30/06	1.23	0.40	24.02	14.57	59.77	15.37
AB22028	Medium Drag	09/20/06	3.09	1.09	18.28	29.15	48.39	31.08

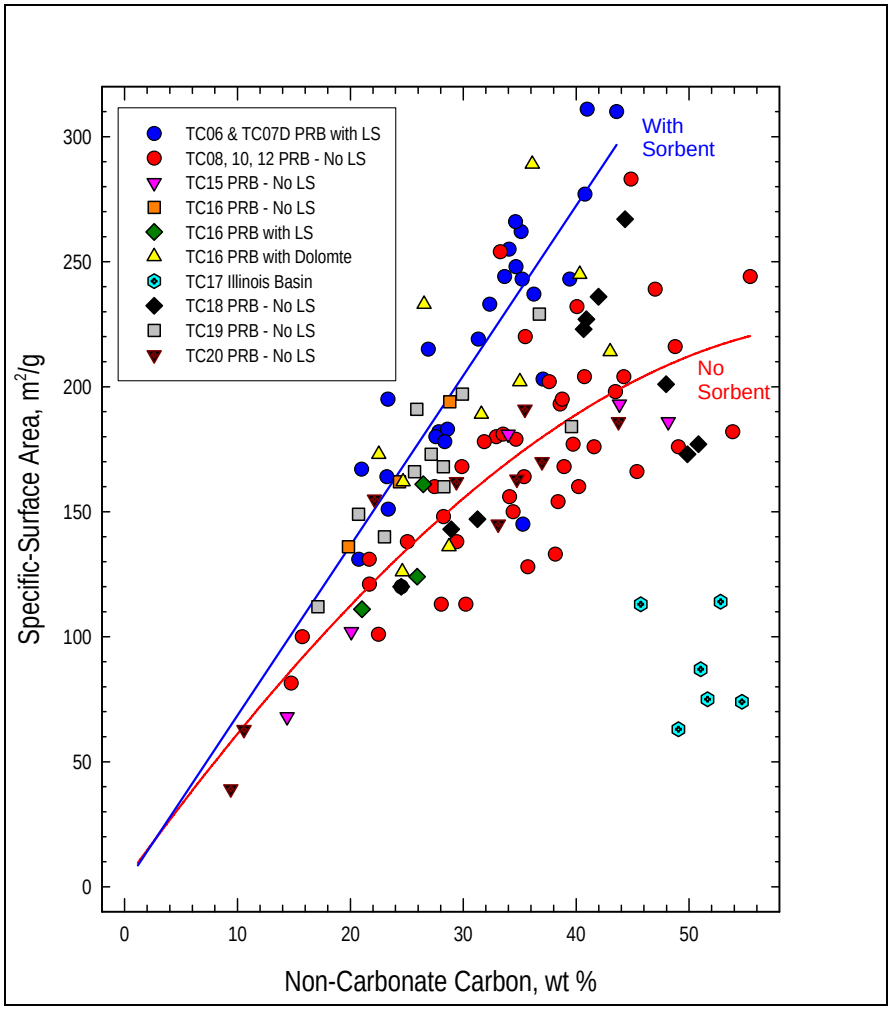

Figure 5-6. Effect of Carbon Content on Specific Surface Area of Gasification Ash.

Dustcake Samples. Tables 5-5 and 5-6 give the physical properties and chemical composition of the dustcake samples taken after the shutdown on August 21, 2006, and after the final shutdown of TC20 on September 26, 2006. The sample from August 21 was collected through the PCD manway after a dirty shutdown. The samples from September 26 were scraped off the filter elements after a semi-dirty shutdown to preserve the entire dustcake on the top plenum and only the residual dustcake on the bottom plenum. The data on the September 26 samples shows a surprising similarity between the transient and residual dustcakes. In previous testing, the residual dustcake had a finer particle size than the transient dustcake and this was explained in terms of a gradual enrichment of the fine-particle fraction that occurs as each backpulse re-entrains some fine particles that are subsequently recollected into the residual dustcake. The TC20 data did not indicate this fine-particle enrichment.

Table 5-5. Physical Properties of Dustcake Samples.

Sample ID	Sample Date	Bulk Density g/cc	True Density g/cc	Uncompacted Bulk Porosity %	Specific Surface Area m^2/g	Mass-Median Diameter mm	Loss on Ignition Wt %
Bulk Dustcake from Dirty Shutdown, Sampled 8/21/06							
AB21260	08/21/06	0.21	2.78	92.4	104	7.3	17.7
Transient + Residual Cake from Top Plenum, Sampled 9/26/06							
AB21938	09/26/06	0.19	2.64	92.8	169	10.0	30.7
Residual Cake from Bottom Plenum, Sampled 9/26/06							
AB21939	09/26/06	0.19	2.62	92.7	165	12.6	28.4

Table 5-6. Chemical Composition of Dustcake Samples.

Sample ID	Sample Date	$CaCO_3$ Wt %	CaS Wt %	CaO Wt %	Non-Carbonate Carbon Wt %	Inerts (Ash/Sand) Wt %	Loss on Ignition Wt %
Bulk Dustcake from Dirty Shutdown, Sampled 8/21/06							
AB21260	8/21/06	1.48	0.43	18.74	16.40	62.95	17.74
Transient + Residual Cake from Top Plenum, Sampled 9/26/06							
AB21938	9/26/06	2.32	0.96	13.56	29.24	53.92	30.73
Residual Cake from Bottom Plenum, Sampled 9/26/06							
AB21939	9/26/06	2.32	1.01	13.15	27.19	56.34	28.43

5.2.4 PCD Pressure Drop Performance

5.2.4.1 Transient PCD Drag

The pressure rise within a cleaning cycle of the PCD is a direct measure of the characteristics of the particulate being collected at that time. Under stable operation the vast majority of this particulate is removed from the filter elements during cleaning so this is referred to as the transient pressure drop. Since pressure drop is a function of the gas velocity, temperature (gas viscosity), particulate loading, and the flow resistance of the particulate, describing PCD operation in terms of pressure drop makes comparison of different conditions and particulate difficult. Instead, a value of normalized drag was calculated, and which is pressure drop normalized to one ft/min face velocity, one lb/ft^2 areal particulate loading, and gas viscosity of air at 70°F. The result is a fundamental parameter that describes the flow resistance of the collected dustcake.

During each in-situ sampling run at the PCD inlet, the PCD transient drag was calculated using the measured particle concentration along with the pressure drop increase and face velocity during the period of the in-situ test. All of the particulate measured at the PCD inlet is assumed to be collected on the filter elements and to contribute to pressure drop. As discussed previously, this assumption is supported by the good agreement between the measured transient dustcake areal loading and the measured PCD inlet solids loading at the end of TC20.

The inputs and results of the transient drag calculations are presented in Table 5-7. The calculated transient drag at PCD conditions is listed under the column heading “PCD.” The corresponding value of transient drag normalized to the viscosity of air at 70^oF is listed under the heading “PCD@RT”. These values are comparable to the lab drag measurements discussed in a later section and are also comparable to other test campaigns that operated at different temperatures.

Normalized PCD transient drag is plotted as a function of time (actually test number) in Figure 5-7 and as a function of carbon content in Figure 5-8. The dashed line in Figure 5-7 is a linear regression to the data. The drag result for Test Number 13 was excluded as an outlier. As discussed in the previous discussion of the particle size distribution changes throughout TC20, the drag responded as expected with decreasing drag with time. Regardless of the cause of the increased particle size, the result is favorable for the PCD. The regression indicates that the drag was reduced by about a factor of two through the length of the test campaign. As seen in previous test campaigns, transient drag also increases with increasing carbon content in the gasification ash. This correlation (Figure 5-8) shows a lot of scatter in the data, because it does not take into account the effect of particle size.

Table 5-7. Transient Drag Determined from PCD Pressure Drop and from Lab Measurements.

Run No.	ΔP/Δt, inwc/min	Δ(AL)/Δt, lb/ft^2/min	FV, ft/min	MMD, μm	LOI, %	Drag, inwc/(lb/ft^2)/(ft/min)		
						PCD	PCD@RT	Lab
9	2.41	0.011	4.10	6.8	34.4	226	133	140
10	1.16	0.006	3.36	5.4	17.5	180	105	144
11	0.88	0.006	3.24	6.2	11.5	140	83	115
12	1.06	0.007	2.61	8.4	28.6	144	86	103
13	3.25	0.010	4.19	5.9	44.9	322	190	188
14	1.67	0.009	3.37	6.8	34.5	194	114	140
15	2.50	0.013	3.71	7.3	37.1	199	116	134
16	2.08	0.012	3.50	6.7	40.8	181	106	155
17	0.55	0.006	2.95	7.1	12.5	87	53	100
18	0.44	0.006	2.96	5.8	10.1	78	47	121
19	1.08	0.010	3.46	10.0	27.4	112	68	84
20	1.66	0.014	4.23	8.3	37.5	120	72	117
21	1.00	0.011	2.94	9.9	28.6	95	57	86
22	1.15	0.012	2.79	11.2	30.1	100	60	77
23	2.24	0.016	4.22	8.6	37.1	143	86	112
24	1.95	0.014	4.75	8.9	35.5	136	82	106
25	1.24	0.012	2.87	8.1	35.9	103	63	118
26	0.65	0.009	2.79	10.3	21.7	73	44	75
27	0.73	0.009	2.99	11.1	22.2	85	51	70
28	0.91	0.009	2.95	9.4	25.6	106	64	88
29	1.71	0.014	3.52	7.2	29.4	127	77	123
30	0.94	0.010	2.76	13.1	26.2	92	55	61
31	1.54	0.015	2.66	10.0	40.4	103	63	100
32	1.13	0.014	2.79	10.5	33.2	81	49	86
33	1.38	0.014	2.86	12.6	38.3	100	61	75
34	0.88	0.011	2.70	10.8	30.9	77	48	81
Avg	1.39	0.011	3.28	8.7	29.7	131	78	108

Lab drag data calculated from linear regression to MMD and LOI of lab drag samples.

Nomenclature:
ΔP/Δt = rate of pressure drop rise during particulate sampling run, inwc/min.
Δ(AL)/Δt = rate of increase in areal loading during sampling run, lb/min/ft2.
FV = average PCD face velocity during particulate sampling run, ft/min.
MMD = mass-median diameter of in-situ particulate sample, μm.
NCC = non-carbonate carbon. LOI = Loss On Ignition.
RT = room temperature, 77°F (25°C).

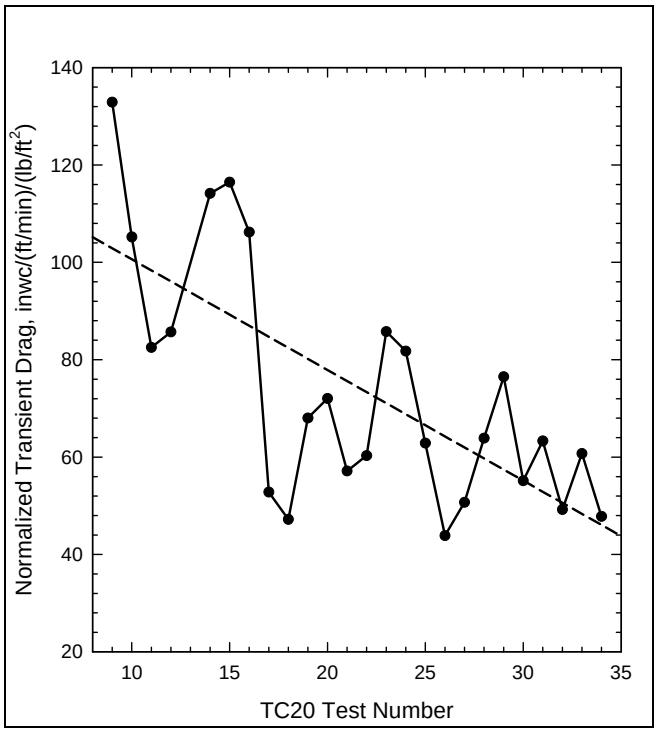

Figure 5-7. Change in PCD Drag with Time.

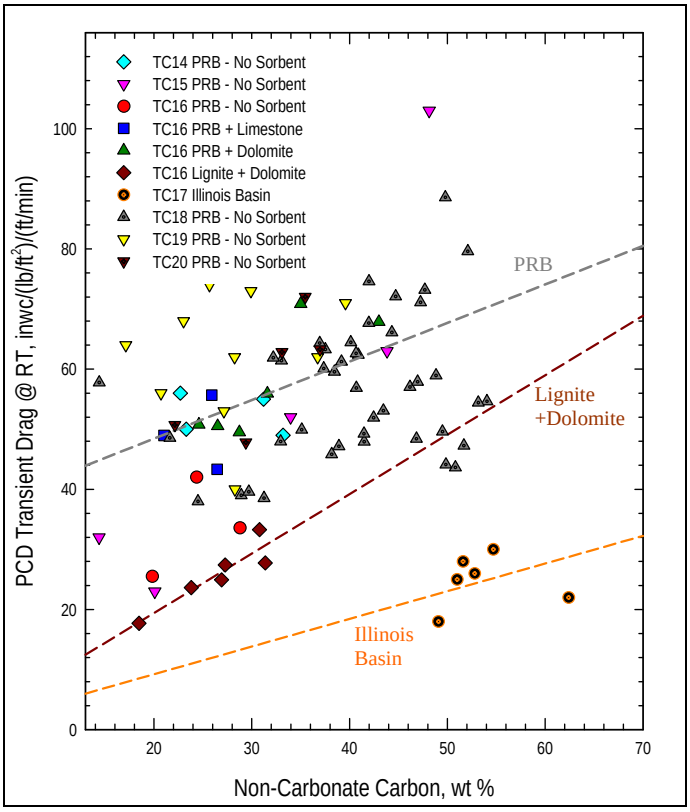

Figure 5-8. PCD Transient Drag versus Carbon Content of In-Situ Samples.

5.2.4.2 Baseline Pressure Drop Analysis

Figure 5-9 depicts the peak and baseline PCD pressure drop for the TC20 test campaign, while the TC20 baseline data are compared to previous test campaigns in Figure 5-10. Both baseline and peak pressure drop increased more rapidly before the outage on August 18, 2006, than they did afterward. This also corresponds to the time period when the size distribution changed the most dramatically. The TC20 baseline pressure drop in Figure 5-9 was considerably lower than the pressure drop values for the last two test campaigns with PRB coal, although the drag of the TC20 particulate was higher and the residual dustcake thickness (Table 5-2) was about the same as previous tests. However, as indicated in Table 5-2, the areal loading of the TC20 residual dustcake was about half that of previous residual dustcakes formed from PRB coal. The lower areal loading of the residual dustcake may have contributed to the lower baseline pressure drop.

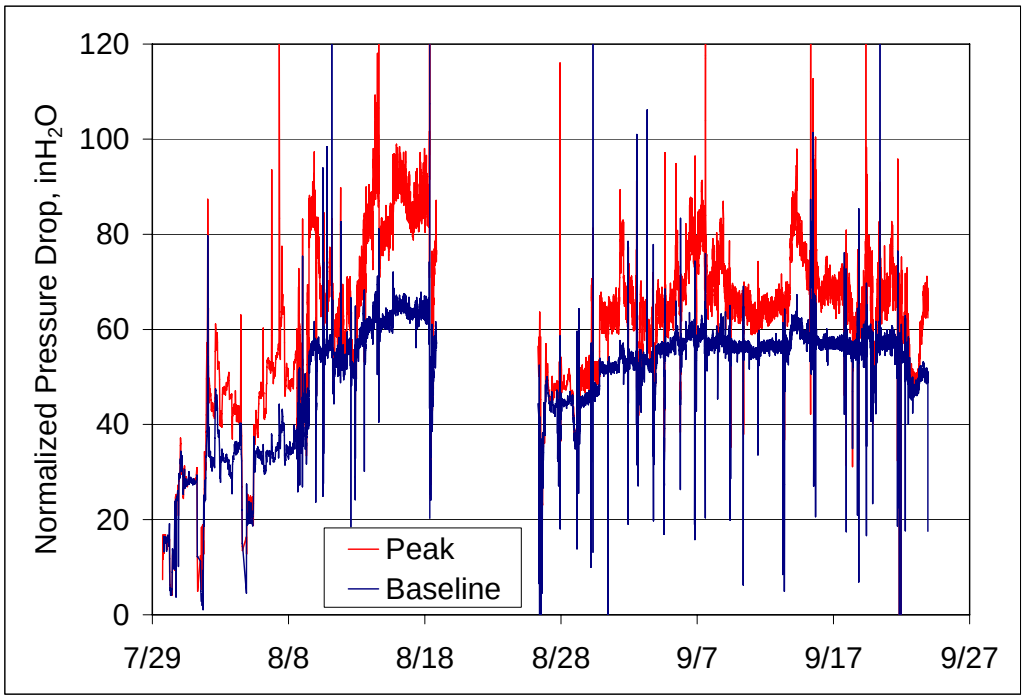

Figure 5-9. Normalized PCD Pressure Drop.

Some of the reduced baseline pressure drop could be attributed to the greater filtering surface area produced by installing a 90 elements in the PCD for TC20 rather than the 72 elements used in the last few test campaigns. Although the data were normalized for face velocity, there are effects on areal loading that may not be accounted for. The much lower inlet loading with the new gasifier configuration will lower the apparent baseline pressure drop. (Since the two plenums are not backpulsed at the same time, a true baseline pressure drop is not obtainable). Another probable cause of lower baseline pressure drop is the large number of low-pressure-drop Dynalloy metal fiber filter elements installed in TC20 versus almost entirely high-pressure-drop iron aluminide sintered powder elements in previous tests. Many of the iron aluminide elements had corrosion that increased the pressure drop more than it would have been with new filter elements.

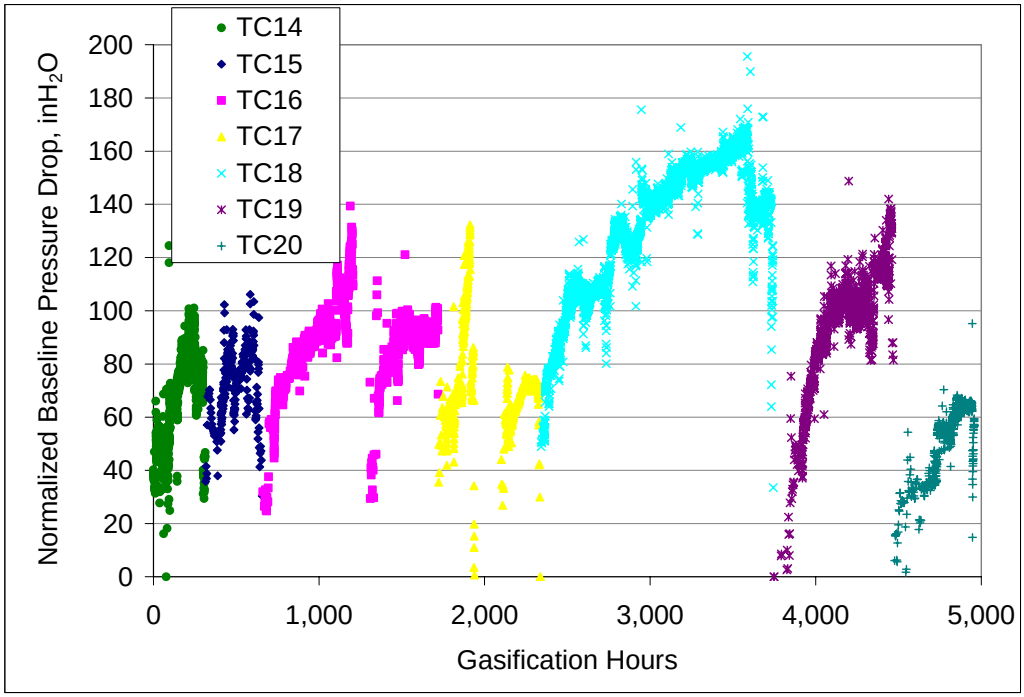

Figure 5-10. Normalized PCD Pressure Drop from TC14 through TC20.

5.2.5 Prediction of PCD Drag and Pressure Drop

5.2.5.1 Lab Drag Measurements

To investigate the characteristics of the TC20 particulate more completely, drag measurements were made in the lab flow resistance test device on the three hopper samples described previously. This lab apparatus uses a series of cyclones between the particulate generator and the dustcake collection surface to vary the particle size distribution of the dustcake. The results are illustrated in Figure 5-11 with normalized drag plotted against the MMD particle size of the collected dustcake. The actual data points are indicated by the triangles and squares, while the solid lines are linear regressions to the data to illustrate the linearity of the results.

In the past, a value of non-carbonate carbon (NCC) for each lab and in-situ sample has been calculated. However, because of the small size of some of the samples and the great number of samples collected in TC20, loss-on-ignition (LOI) was used as a proxy for NCC in TC20. As shown in the previous tables of chemical properties, the values of NCC and LOI were very similar in TC20. This would not be the case if calcium based sorbents were added to the gasifier, but no sorbents were used in TC20.

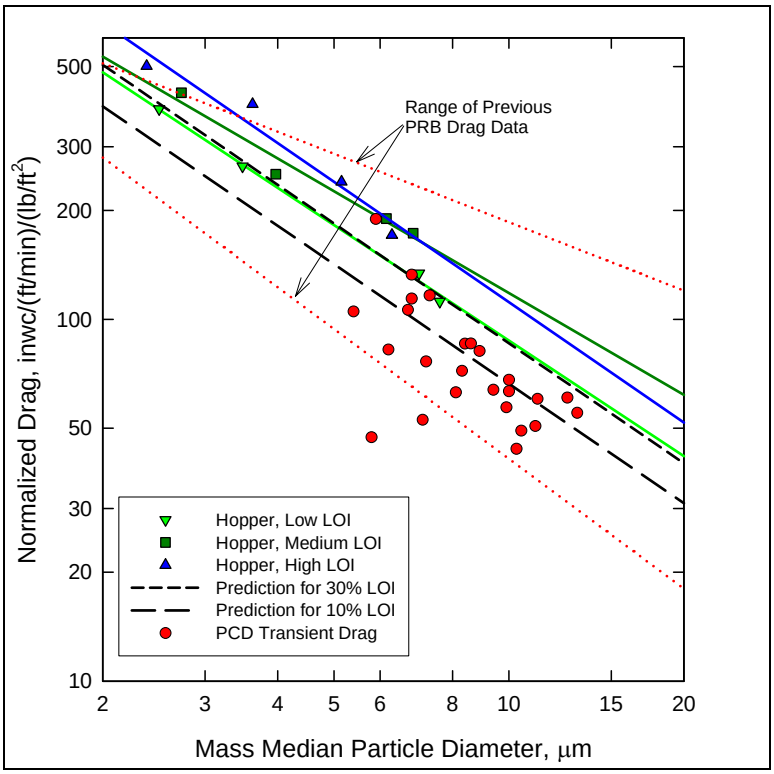

Figure 5-11. Lab-Measured Drag as a Function of Particle Size.

The LOI values for the three bulk lab drag samples were 15 percent (low LOI), 31 percent (medium LOI), and 39 percent (high LOI). The lab drag values generally indicated increasing drag with increasing carbon content, although there was some overlap with the 31 percent and 39 percent samples. The reason for the overlap between the medium and high LOI samples may be related to their surface areas. The TC20 samples showed a more pronounced effect for drag versus particle size with greater slope than observed in TC19. The dotted lines on the graph represent the range of PRB drag data measured previously, and the TC20 lab data fell toward the middle of this range for large particles, but set a new high for small particles.

The solid circle symbols on the graph (Figure 5-11) are the values of PCD transient drag calculated for each of the in-situ samples from Table 5-7. Many of the PCD data points fell below the lab drag measurements despite similar values of bulk carbon. As observed in TC19, the carbon contents of the samples collected in the lab device were considerably higher (more than twice as high in some cases) than the bulk samples they were derived from. The increased carbon content was greatest for the largest particle fractions, while the 2 to 3 micron fraction had less carbon elevation. A multiple linear regression was calculated between the drag, MMD, and LOI of each of the eight individual lab drag samples. (The old technique was not used with these data.) This regression calculation produced the following equation:

$$\text{Drag} = 10\text{^}(2.860 - (1.093 * \text{Log}(\text{MMD})) + 0.00572 * \text{NCC}), \text{ with an } r^2 = 0.98.$$

The regression equation reflects the increased slope of drag as a function of particle size (slope of 1.09 in TC20 versus 0.66 in TC19), while the effect of carbon content was essentially the same for both test campaigns.

The regression was used to calculate drag versus particle size with two different carbon contents that are equal to the minimum and average carbon contents of the in-situ samples, 10 percent and 30 percent LOI, respectively. These predictions are shown on Figure 5-11 as the dashed lines. Although not in perfect agreement, the predictions made from the regression technique match the PCD data reasonably well.

The results of regression predictions for each individual value of PCD transient drag are shown in Table 5-7. These calculations used the MMD and LOI of each in-situ sample to predict the transient drag of the PCD during that test. The lab predictions were higher than the actual PCD data for both the individual values and the average for TC20.

5.2.5.2 Comparison of Lab Measurements with Transient Drag

Average lab and PCD drag values for all gasification test campaigns are summarized in Table 5-8. The comparison indicates excellent overall historical agreement (average difference of about 10 percent), even though the difference was much higher for certain test campaigns. For TC20, the difference was 32 percent. The results for all gasification test campaigns are plotted in Figure 5-12 and continued to show scatter around the perfect agreement line. The average value of TC20 drag measured in the lab (108 inwc/(lb/ft^2)/(ft/min)) was the highest measured for any test campaign to date. The actual TC20 PCD drag value of 78 inwc/(lb/ft^2)/(ft/min) was the third highest ever measured. These high drag values were consistent with the finer particle size distributions resulting from the increased collection efficiency of the new gasifier solids separation unit. The reduced dustcake loading caused by the lower particulate concentrations should tend to negate some of this effect to limit PCD pressure drop.

Table 5-8. Average Drag Values Determined from PCD and Lab Measurements

Run	Coal	Average Transient Drag Determined from PCD Performance, inwc/(lb/ft^2)/(ft/min)	Average Drag Determined from RAPTOR Lab Measurements, inwc/(lb/ft^2)/(ft/min)	Difference from Mean Value*, %
GCT2	PRB	29.3	20.9	-33.5
GCT3	PRB	80.2	92.7	14.5
GCT4	PRB	66.4	57	-15.2
TC06	PRB	89.4	81.2	-9.6
TC07	PRB	47.7	49.8	4.3
TC08	PRB	46.5	50	7.3
TC09	Hiawatha	29.0	23.3	-21.8
TC10	PRB	44.7	57.6	25.2
TC11	Falkirk Lignite	16.1	35.9	76.2
TC12	PRB	58.0	60.8	4.7
TC13	Freedom Lignite	34.4	39.4	13.6
TC14	PRB	47.4	41.6	-13.0
TC15	PRB	54.6	76.4	33.3
TC16	PRB + Limestone	49.3	51.7	4.8
TC16	Lignite + Dolomite	25.8	41.7	47.1
TC17	IL Basin	24.8	18.7	-27.8
TC18	PRB	59.0	82.0	32.6
TC19**	PRB	64.0	72.0	11.8
TC20**	PRB	78.0	108.0	32.3
Average		49.7	55.8	9.8

* D = (R1-R2)/(R1+R2)/2*100
** Technique modified to use carbon content of lab drag sample

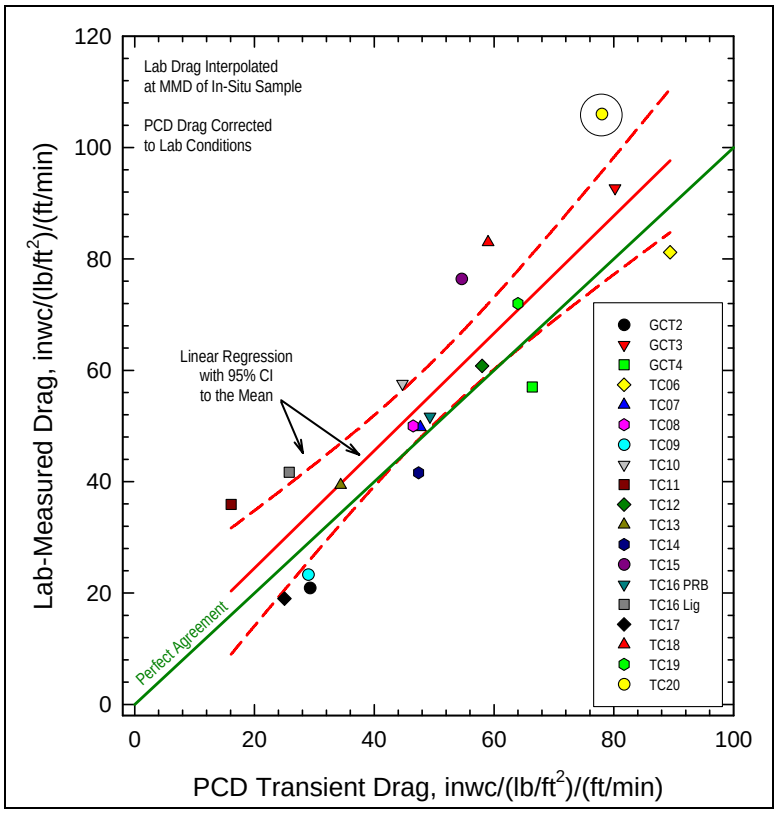

Figure 5-12. Comparison of PCD Transient Drag with Lab Measurements.

5.2.6 Analysis of PCD Filter Element Condition

At the end of TC20, the PCD was partially disassembled to analyze the condition of the filter elements. Because of a short turn-around time planned between TC20 and TC21, only eight filter elements were removed for testing and analysis.

At the end of TC20, the top plenum was not backpulsed clean after coal feed was stopped. This is referred to as a “dirty shutdown” for the top plenum. For the first time, some filter elements were removed and transported to the flow test facility without disturbing the transient dustcake. The pressure drop versus flow was measured for these filter elements in the following conditions:

- With the transient plus residual dustcake
- With an approximation of the residual dustcake by simulated back pulsing
- After air blowing the filter surface (old standard flow test technique)
- After pressure washing to remove all particulate

The results were largely unremarkable except for the illustration of the effect of any dustcake on the extensively tested filter elements that have corrosion product. Figure 5-13 shows the results for the oldest iron aluminide element, which had 8,527 hours in gasification, while Figure 5-14 is for another iron aluminide element with only 1,369 hours of use in gasification. Only minor differences were seen between the transient, residual, and embedded dustcakes for either element type. That is, the change in pressure versus flow as each particulate layer was removed was the same for both old and young filter elements, although the old filter had much higher absolute values of pressure drop. However, the difference in pressure drop from removing the embedded dustcake from the older filter was dramatically greater than for the young iron aluminide element. This effect was discussed in the TC19 report for a large number of filter elements. That type of graph cannot be reproduced for the TC20 data because of the small number of data points collected for this test campaign.

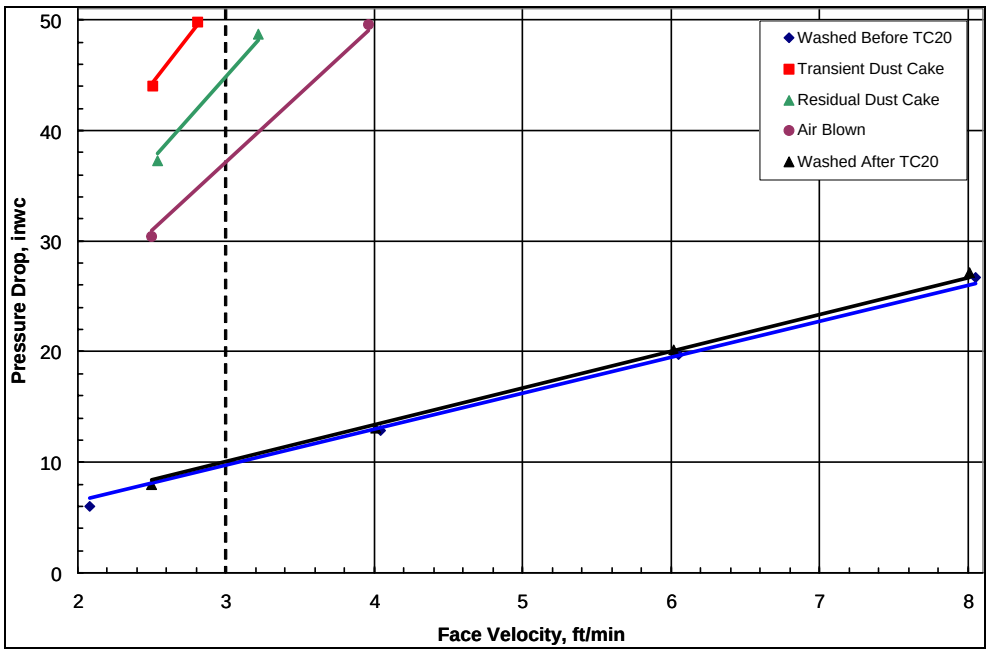

Figure 5-13. Pressure Drop versus Face Velocity of Iron Aluminide Filter Element with 8,527 Exposure Hours.

Figure 5-15 shows the same type of flow test results for a Dynalloy HR-160 filter with about the same number of hours as the young iron aluminide filter. The results are similar for both young filter elements except that the Dynalloy filter elements had lower clean pressure drop, which propagated through all of the pressure drop values.

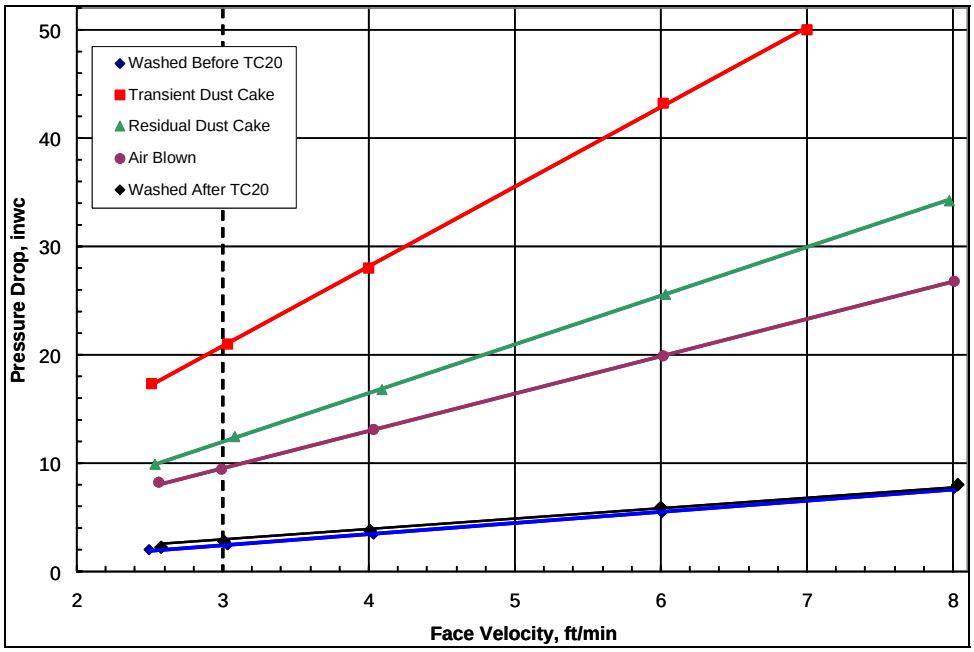

Figure 5-14. Pressure Drop versus Face Velocity for Iron Aluminide Filter Element with 1,369 Exposure Hours.

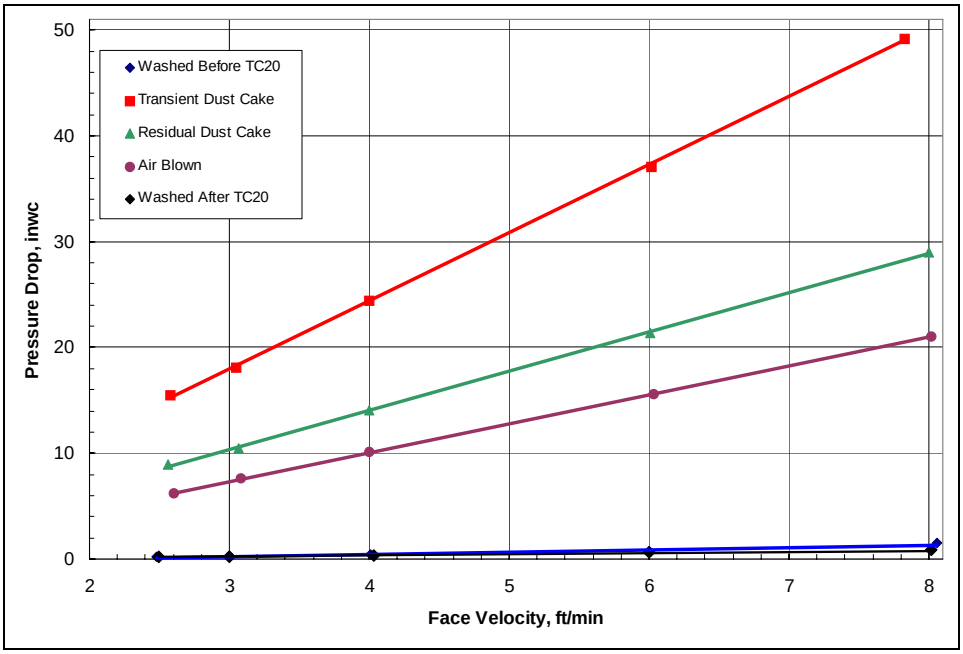

Figure 5-15. Pressure Drop versus Face Velocity for Dynalloy HR-160 Filter Element with 1,595 Hours.

6.0 ADVANCED SYNGAS CLEANUP

The advanced syngas cleanup unit was used in TC20 for testing of COS hydrolysis catalysts and syngas cooler fouling. The COS hydrolysis testing utilized five different types of COS catalysts. Syngas cooler fouling was evaluated while temperatures were lowered below the dew point of the syngas stream. Gas analysis was performed using FTIR and gas chromatography with flame photometric detection.

6.1 COS Hydrolysis Testing

The COS hydrolysis catalysts were supplied by Sud-Chemie, Engelhard, Johnson Matthey, and Alcoa. Aluminum oxide was the basic material of the catalysts, with proprietary amounts of additional materials. The testing was performed in 310 stainless steel reactors with 5.2 inch inner diameters and heights of 5 feet. Space velocity was maintained at 2000/hr. Nominal catalyst properties and operating parameters for the COS hydrolysis tests are shown in Table 6.1. The COS conversions ranged from 80 to 93 percent.

Table 6.1. COS Hydrolysis Catalyst Properties and Nominal Operating Parameters.

Catalyst Supplier	Sud-Chemie	Engelhard	Johnson Matthey	Alcoa	Alcoa
Catalyst Type	C53-2-01	Selexcat	Puraspec 2312	Selexsorb	F200
Physical Properties					
Aluminum Oxide Content, wt %	--	84-96	100	84-96	94-100
Shape	Extrusion	Spheres	Spheres	Spheres	Spheres
Size, mm	3.2	2	3	3.7	3.2
Density, lb/ft^3	30	45.6	43.7	46.8	43.1
Catalyst Bed Mass, lb	6.5	9.8	9.4	10.1	9.3
Catalyst Bed Height, in	17.7	17.6	17.6	17.6	17.6
Operating Parameters					
Pressure, psig	190	225	180	165	180
Temperature, ^{o}F	420	390	390	400	420
Inlet COS Concentration, ppm	22.5	26.5	27.0	23.5	22.9
Outlet COS Concentration, ppm	4.5	1.7	2.3	4.3	2.4
COS Conversion	80	93	92	82	90
Operating Time, hr	92	120	101	58	130

6.2 Syngas Cooler Fouling Testing

The syngas cooler on the advanced syngas cleanup slipstream was operated for a period of 300 hours to cool syngas using a recirculating loop chiller so that the condensate from the syngas could be collected. The syngas flow through the cooler was maintained at 30 lb/hr. The syngas cooler inlet temperature was approximately 500ºF, and the outlet temperature was approximately 120ºF. Gas velocity through the cooler tube was 49 ft/sec. Exchanger tube fouling with organics was observed when the chiller water inlet temperature was lowered to 50ºF. The condensate collected was transparent. Future testing will evaluate syngas cooler fouling at high pressures.

7.0 CONCLUSIONS

A major focus of test campaign TC20 was characterization of the gasifier modifications completed in 2006. These modifications were the most significant changes to the PSDF Transport Gasifier since its installation in 1996. The purpose of the modifications was to improve residence time and solid collection efficiencies, two critical parameters for expansion of the fuel operating envelope and commercialization of gasification technology. Test data indicated a marked improvement in both parameters. In addition to evaluating gasifier modifications, several other objectives were achieved during TC20, all directed related to development of commercially viable gasification technologies. Further advancements in gasification technologies will be built on the accomplishments realized in TC20.

Lessons Learned. The main points gained from TC20 operation are listed below.

- Operation of the new dispense vessel vent valve on the original coal feeder resulted in decreased frequency of vent line plugging compared to previous test campaigns.
- In designing the new gasifier configuration, cold flow modeling was performed to develop the design equations based on first principles. Testing confirmed the design equations developed from cold flow modeling. Thus, the uncertainty in scale-up of the first stage separation device was substantially reduced.
- Efficiency of the first gasifier solids separation unit improved significantly, increasing from less than 85 percent to greater than 99 percent. Solids physical and chemical analyses confirmed that the first collection device accounted for the majority of solids collection in the gasifier.
- The modified solids separation unit was more efficient in collecting the larger particles of gasification ash than was the previous configuration.
- Significant syngas quality enhancements also indicated improved gasifier residence time and collection efficiency. The syngas lower heating values increased by about 10 to 20 percent compared to previous PRB testing.
- Test data demonstrated a positive correlation between the syngas heating value and coal feed rate.
- The circulation rate showed a fairly linear relationship with the standpipe level.
- The average particle size of the gasifier circulating solids decreased about 56 percent, and the particulate carried over to the PCD also become significantly finer, indicating a 55 percent reduction in average particle size. The improved gasifier solids collection efficiency resulted in an average PCD inlet solids mass rate that was about 30 percent less than seen in previous test campaigns.
- While the collection efficiency of the Dynalloy HR-160 PCD filter elements was not as high as that of the iron aluminide elements, the HR-160 elements demonstrated adequate collection efficiency with less evidence of corrosion.
- On-line testing of a new failsafe media configuration showed promising results in preventing particulate penetration in the event of a PCD element failure.
- Transport air for coal conveying was used successfully for 290 hours and resulted in a higher syngas heating value.

- Testing of anhydrous ammonia injections to the gasifier showed no increase in the gasifier outlet ammonia concentration, indicating ammonia decomposition in the gasifier. Measurements of NOx sampled at the atmospheric syngas combustor outlet did not indicate an increase in NOx during the injections.
- Measurements from the SGC05 design of ceramic-tipped PDIs tested in the gasifier compared well with standard PDI measurements. Measurements from the MAC10 design did not compare as well with the standard measurements, but the agreement was considered fair given the variability of density in the areas measured.
- There were no gasifier thermocouple failures during TC20. Thermocouple durability was improved over previous test campaigns likely due to the decreased particle size and decreased solids velocity in the gasifier resulting from the modifications.

APPENDIX A OPERATING HISTORY

System commissioning of the KBR Transport Reactor train and the first five test campaigns (TCs) were performed in combustion mode. Approximately 5,000 hours of combustion operation were completed from 1996 to 1999. The system was transitioned to gasification operation in late 1999. Four gasification commissioning tests (GCTs), each lasting nominally 250 hours, were completed by early 2001. At the conclusion of TC20, 15 gasification test campaigns were completed, each nominally 250 to 1,500 hours in duration, for a total of about 9,150 hours of coal gasification operation. Powder River Basin subbituminous coal is the most extensively tested fuel, although several bituminous and lignite coals have also been tested. The Transport Gasifier has operated successfully in both air-blown and oxygen-blown modes.

Table A-1 summarizes the gasification testing completed at the conclusion of TC20. The table lists the number of hours on coal, fuel type, and major objectives of each test. More information about the individual test campaigns may be found in the test campaign reports, located on the PSDF website, http://psdf.southernco.com.

Table A-1. Gasification Operating History.

Test	Start Date	Duration (hrs)	Fuel Type*	Comments
GCT1	September 1999	233	PRB, Illinois #6, Alabama	First gasification testing
GCT2	April 2000	218	PRB	Stable operations
GCT3	February 2001	184	PRB	Loop seal commissioning
GCT4	March 2001	242	PRB	Final gasification commissioning test
TC06	July 2001	1,025	PRB	First long duration test campaign
TC07	April 2002	442	PRB, Alabama	Lower mixing zone commissioning
TC08	June 2002	365	PRB	First oxygen-blown testing First on-line failsafe testing
TC09	September 2002	309	Hiawatha	New mixing zone steam system
TC10	October 2002	416	PRB	Developmental coal feeder
TC11	April 2003	192	Falkirk Lignite	First lignite testing
TC12	May 2003	733	PRB	Fuel cell testing
TC13	September 2003	501	PRB, Freedom Lignite	Syngas to combustion turbine
TC14	February 2004	214	PRB	Syngas to combustion turbine CFAD commissioning
TC15	April 2004	200	PRB	Improved oxygen feed distribution
TC16	July 2004	835	PRB, Freedom Lignite	Fuel cell testing High pressure O_2-blown operation
TC17	October 2004	313	PRB, Illinois Basin	Bituminous coal testing
TC18	June 2005	1,342	PRB	Recycle gas compressor commissioning
TC19	November 2005	518	PRB	CCAD commissioning
TC20	August 2006	870	PRB	Gasifier configuration modifications

*Note: PRB is subbituminous coal; Illinois #6, Alabama, Hiawatha, and Illinois Basin coals are bituminous coals.

APPENDIX B STEADY STATE OPERATING PERIODS AND MAJOR OPERATING PARAMETERS

Test campaign TC20 consisted of 70 steady state periods of operation, which comprised 418 hours, or 48 percent of the total on-coal operating time. The duration of the steady state periods was typically three hours or more, with the average period lasting six hours. During these periods, the coal, steam, and air/oxygen feed rates, operating pressure and temperature, carbon conversion, and syngas lower heating values were generally constant.

Table B-1 lists the operating periods as well as the operating parameters for each period. The coal feed rates were derived from the coal feeder weigh cell data, and the air, oxygen, and syngas flow rates were taken from flow indicators. The steam flow rates were taken from the flow indicators when the instruments were operating reliably (periods TC20-19 to -53, TC20-55 to -58, TC20-65, TC20-69, and TC20-70) and were calculated from a hydrogen balance for the remainder of the operating periods. Nitrogen rates were corrected for ash transport nitrogen and for the secondary coal feeder conveying nitrogen. The original coal feeder was used throughout TC20 except for periods TC20-5 and -6, when the secondary feeder was used exclusively for coal feed. Both feeders were used during periods TC20-7 through -9. Air was used in place of nitrogen as the coal transport gas with the original coal feeder during operating periods TC20-32 through -48 and TC20-56 through -68. The PCD solids rates were interpolated between measured PCD solids rates during in-situ PCD inlet sampling, and the gasifier ash removal rates were calculated by an ash balance.

Table B-1. Steady State Operating Periods and Major Operating Parameters.
(Page 1 of 2)

Operating Period	Start Time	End Time	Run Time Hours	Gasifier Outlet Temperature °F	Gasifier Outlet Pressure psig	Coal Feed Rate lb/hr	Air Feed Rate lb/hr	Oxygen Feed Rate lb/hr	Steam Feed Rate lb/hr	Nitrogen Flow Rate lb/hr	Syngas Rate lb/hr	PCD Inlet Temperature °F	Gasifier Solids Removal Rate lb/hr	PCD Solids Removal Rate lb/hr
TC20-1	8/10/2006 2:15	8/10/2006 7:30	27	1,680	210	3,920	13,320	0	1,010	5,790	23,820	790	140	120
TC20-2	8/10/2006 7:30	8/10/2006 12:30	32	1,700	210	3,820	13,250	0	1,100	5,540	23,340	800	140	100
TC20-3	8/10/2006 15:00	8/10/2006 19:30	39	1,700	210	3,720	13,050	0	1,140	5,370	22,860	800	140	100
TC20-4	8/10/2006 20:30	8/11/2006 1:00	45	1,700	210	3,850	13,040	0	980	5,240	22,990	800	160	100
TC20-5	8/11/2006 9:45	8/11/2006 12:45	57	1,710	190	3,670	11,770	0	960	5,160	21,370	790	130	100
TC20-6	8/11/2006 13:00	8/11/2006 17:00	61	1,710	190	3,110	10,900	0	960	5,330	20,320	780	100	100
TC20-7	8/12/2006 7:30	8/12/2006 12:45	80	1,650	250	3,430	11,260	0	1,240	6,800	21,680	770	120	120
TC20-8	8/12/2006 17:00	8/12/2006 21:00	89	1,700	260	2,700	9,960	0	1,240	6,640	19,120	760	60	130
TC20-9	8/13/2006 1:30	8/13/2006 4:30	97	1,700	260	3,790	13,100	0	1,230	6,950	24,210	800	110	140
TC20-10	8/13/2006 17:30	8/13/2006 20:30	113	1,710	180	4,420	14,460	0	1,190	4,820	25,050	810	150	150
TC20-11	8/14/2006 5:00	8/14/2006 9:30	125	1,670	180	4,470	14,300	0	960	4,800	24,860	800	160	160
TC20-12	8/14/2006 16:00	8/14/2006 20:45	136	1,660	230	4,470	14,170	0	1,390	4,770	25,580	800	170	150
TC20-13	8/14/2006 21:00	8/15/2006 5:45	143	1,670	230	4,450	14,160	0	1,330	4,810	25,640	800	170	150
TC20-14	8/15/2006 11:00	8/15/2006 15:45	155	1,650	230	4,590	14,200	0	1,320	4,800	25,800	800	180	150
TC20-15	8/15/2006 21:00	8/16/2006 8:30	169	1,670	210	4,700	14,640	0	1,260	4,960	25,990	810	160	190
TC20-16	8/16/2006 8:45	8/16/2006 13:45	177	1,680	210	4,680	14,640	0	1,260	4,590	25,650	810	150	200
TC20-17	8/16/2006 14:30	8/16/2006 19:00	183	1,680	210	4,640	14,770	0	1,370	4,830	25,850	810	150	200
TC20-18	8/16/2006 19:00	8/17/2006 4:30	190	1,690	210	4,710	14,860	0	1,480	4,820	25,980	810	150	190
TC20-19	8/17/2006 8:00	8/17/2006 12:45	200	1,690	210	4,690	14,680	0	1,560	4,250	24,490	800	160	190
TC20-20	8/17/2006 14:00	8/17/2006 19:00	206	1,690	210	4,620	14,520	0	1,600	4,560	24,730	800	160	190
TC20-21	8/17/2006 20:15	8/18/2006 0:30	212	1,690	210	4,610	14,590	0	1,380	4,640	24,900	800	160	190
TC20-22	8/29/2006 16:00	8/30/2006 1:45	251	1,690	160	2,210	9,430	0	1,410	5,040	17,510	730	50	100
TC20-23	8/30/2006 11:30	8/30/2006 15:30	267	1,690	160	2,260	9,350	0	1,340	4,530	16,900	720	50	100
TC20-24	8/30/2006 15:30	8/30/2006 20:00	272	1,700	160	2,220	9,310	0	1,410	4,620	16,910	720	30	120
TC20-25	8/30/2006 21:45	8/31/2006 10:15	282	1,680	160	3,110	11,150	0	1,270	4,640	19,950	740	70	140
TC20-26	8/31/2006 14:45	9/1/2006 6:30	301	1,670	160	3,140	11,140	0	1,270	4,900	20,110	740	50	190
TC20-27	9/1/2006 8:15	9/1/2006 12:30	312	1,680	160	4,230	13,530	0	1,330	4,660	23,300	760	100	220
TC20-28	9/1/2006 16:30	9/1/2006 21:45	321	1,680	220	4,190	13,530	0	1,320	5,160	23,680	760	110	220
TC20-29	9/2/2006 0:45	9/2/2006 5:30	329	1,680	220	4,080	13,380	0	1,280	5,350	23,410	760	110	210
TC20-30	9/2/2006 9:45	9/2/2006 12:30	337	1,720	210	4,110	13,630	0	1,280	4,980	23,910	780	100	210
TC20-31	9/3/2006 3:30	9/3/2006 7:45	356	1,690	210	3,650	12,580	0	1,080	5,230	22,530	760	80	190
TC20-32	9/3/2006 10:30	9/3/2006 15:15	363	1,700	210	3,690	12,740	0	1,060	4,080	21,830	760	80	190
TC20-33	9/4/2006 4:15	9/4/2006 9:00	381	1,700	220	4,110	13,330	0	1,040	3,990	22,570	760	120	170
TC20-34	9/4/2006 9:00	9/4/2006 13:15	385	1,700	220	4,110	13,350	0	1,060	3,810	22,430	760	120	170
TC20-35	9/4/2006 17:00	9/5/2006 0:45	395	1,700	240	4,150	13,560	0	1,010	3,950	23,040	760	120	180

Table B-1. Steady State Operating Periods and Major Operating Parameters.
(Page 2 of 2)

Operating Period	Start Time	End Time	Run Time, Hours	Gasifier Outlet Temperature, °F	Gasifier Outlet Pressure, psig	Coal Feed Rate, lb/hr	Air Feed Rate, lb/hr	Oxygen Feed Rate, lb/hr	Steam Feed Rate, lb/hr	Nitrogen Flow Rate, lb/hr	Syngas Rate, lb/hr	PCD Inlet Temperature, °F	Gasifier Solids Removal Rate, lb/hr	PCD Solids Removal Rate, lb/hr
TC20-36	9/5/2006 1:15	9/5/2006 9:00	403	1,700	230	4,140	13,450	0	1,480	3,960	23,080	760	110	180
TC20-37	9/5/2006 14:00	9/5/2006 18:15	414	1,700	210	4,280	13,730	0	1,560	4,230	23,640	770	90	200
TC20-38	9/5/2006 20:15	9/6/2006 3:30	422	1,710	200	4,240	14,020	0	1,600	4,080	23,970	770	80	220
TC20-39	9/6/2006 12:30	9/6/2006 17:00	437	1,690	160	4,370	13,660	0	1,380	3,830	23,010	750	100	250
TC20-40	9/6/2006 23:15	9/7/2006 12:45	452	1,700	140	4,370	13,940	0	1,410	3,660	23,370	760	110	240
TC20-41	9/7/2006 19:15	9/8/2006 2:15	469	1,680	220	4,220	13,360	0	1,340	3,920	22,580	750	120	210
TC20-42	9/8/2006 2:30	9/8/2006 12:00	477	1,660	220	4,250	13,190	0	1,410	3,830	22,520	740	110	200
TC20-43	9/9/2006 17:45	9/9/2006 21:45	514	1,700	210	3,920	12,860	0	1,270	4,070	21,800	750	120	170
TC20-44	9/9/2006 21:45	9/10/2006 8:45	521	1,700	210	4,020	13,000	0	1,270	4,080	22,030	750	130	170
TC20-45	9/10/2006 10:45	9/10/2006 15:45	531	1,700	210	4,080	13,220	0	1,330	4,000	22,300	750	140	160
TC20-46	9/10/2006 15:45	9/10/2006 21:45	537	1,700	220	4,130	13,270	0	1,320	3,970	22,350	750	120	150
TC20-47	9/10/2006 22:30	9/11/2006 5:00	544	1,710	220	3,870	12,730	0	1,280	4,080	21,500	750	120	150
TC20-48	9/11/2006 5:15	9/11/2006 10:30	550	1,730	220	3,850	13,060	0	1,280	3,800	21,740	760	120	150
TC20-49	9/11/2006 14:45	9/11/2006 18:45	559	1,730	230	3,820	13,270	0	1,080	5,140	22,670	760	130	140
TC20-50	9/11/2006 18:45	9/12/2006 5:30	566	1,730	230	3,980	13,540	0	1,060	5,190	23,100	760	130	140
TC20-51	9/12/2006 5:30	9/12/2006 21:00	579	1,730	230	4,030	13,650	0	1,040	5,210	23,210	760	130	140
TC20-52	9/12/2006 21:45	9/13/2006 1:45	590	1,730	230	4,040	13,650	0	1,060	5,280	23,300	760	130	140
TC20-53	9/13/2006 12:30	9/13/2006 19:15	606	1,720	230	4,040	13,550	0	1,010	5,090	22,970	760	150	150
TC20-54	9/14/2006 0:15	9/14/2006 6:15	617	1,690	220	4,850	14,740	0	1,020	5,170	24,850	750	140	200
TC20-55	9/14/2006 8:45	9/14/2006 13:30	625	1,690	220	4,880	15,210	0	1,770	5,320	26,380	770	130	220
TC20-56	9/14/2006 16:15	9/14/2006 20:15	632	1,710	220	4,750	15,360	0	2,110	4,420	25,890	780	130	210
TC20-57	9/14/2006 20:15	9/15/2006 0:15	636	1,720	220	4,750	15,440	0	2,100	4,380	25,950	790	110	210
TC20-58	9/15/2006 22:30	9/16/2006 2:45	663	1,740	250	4,330	15,520	0	1,360	4,910	26,700	800	130	200
TC20-59	9/16/2006 5:15	9/16/2006 10:15	670	1,750	250	4,390	15,570	0	970	4,760	26,340	790	130	190
TC20-60	9/16/2006 14:15	9/16/2006 19:15	679	1,720	240	4,390	14,650	0	890	5,110	24,190	760	140	190
TC20-61	9/16/2006 23:00	9/17/2006 2:00	687	1,720	250	4,430	14,770	0	1,010	5,300	24,580	770	140	180
TC20-62	9/17/2006 4:00	9/17/2006 9:15	693	1,730	250	4,450	14,900	0	1,030	5,320	24,800	770	140	180
TC20-63	9/17/2006 9:15	9/17/2006 18:00	700	1,730	250	4,410	14,580	0	1,020	5,180	24,310	760	120	180
TC20-64	9/18/2006 5:15	9/18/2006 9:15	717	1,720	240	4,090	14,130	0	950	4,910	23,350	750	90	170
TC20-65	9/19/2006 11:00	9/19/2006 17:15	748	1,610	240	4,220	13,180	0	1,670	4,910	23,660	720	90	240
TC20-66	9/20/2006 12:45	9/20/2006 18:00	773	1,700	240	4,220	13,950	0	910	5,080	23,340	740	100	230
TC20-67	9/20/2006 19:00	9/21/2006 4:00	781	1,710	240	4,340	14,130	0	790	5,220	23,690	750	100	220
TC20-68	9/21/2006 11:00	9/21/2006 15:45	795	1,690	240	4,230	13,940	0	890	5,570	23,750	740	70	220
TC20-69	9/22/2006 22:30	9/23/2006 2:30	830	1,710	160	2,040	800	1,940	3,510	6,570	15,100	730	70	190
TC20-70	9/23/2006 18:00	9/23/2006 22:30	850	1,660	160	3,760	2,580	2,270	2,000	6,970	16,990	720	180	190

APPENDIX C MATERIAL AND ENERGY BALANCES

The material and energy balances showed reasonable accuracy given the diversity of the measurements used for their calculation. The gasifier mass balance for the TC20 steady state operating periods is plotted in Figure C-1. The mass balance documents the accuracy of the solids and gas rates at the inlet and outlet of the gasifier. The data agreed within five percent.

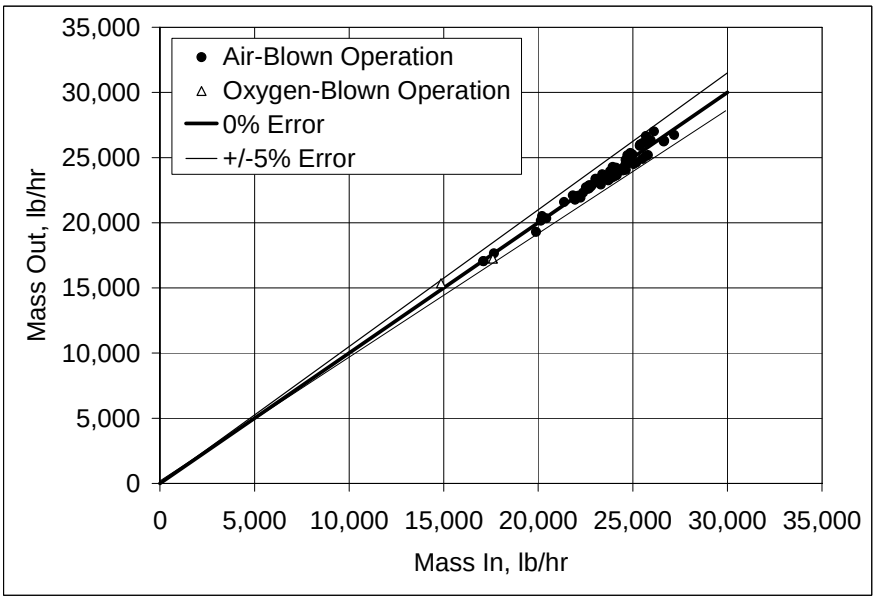

Figure C-1. Mass Balance.

The overall energy balance for the gasifier, presented in Figure C-2, was derived assuming a gasifier heat loss of 3.5 MMBtu/hr. This balance verifies the accuracy of the gasification efficiencies, and shows agreement within a 20 percent error range.

The carbon balance documents the accuracy of the carbon conversions, and is shown in Figure C-3. The data fell within a 20 percent error range

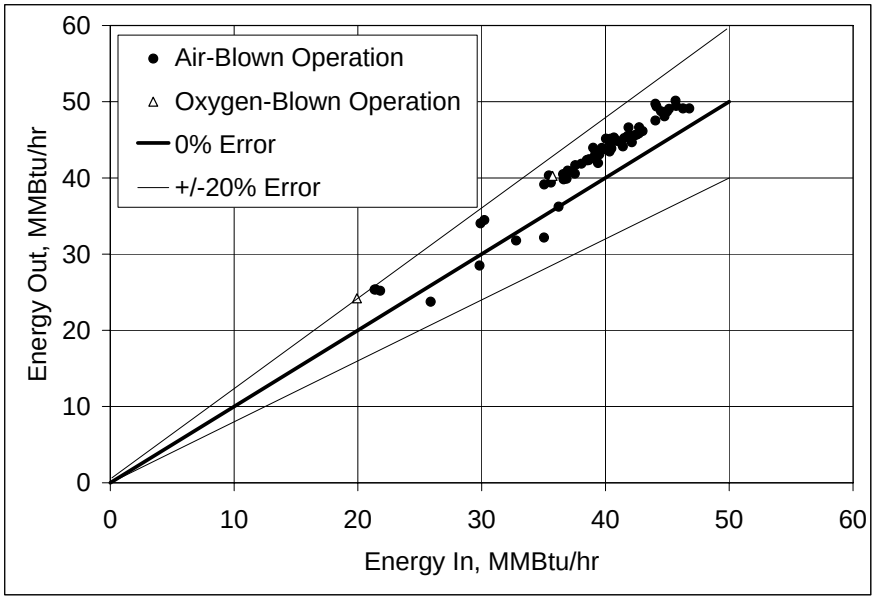

Figure C-2. Energy Balance.

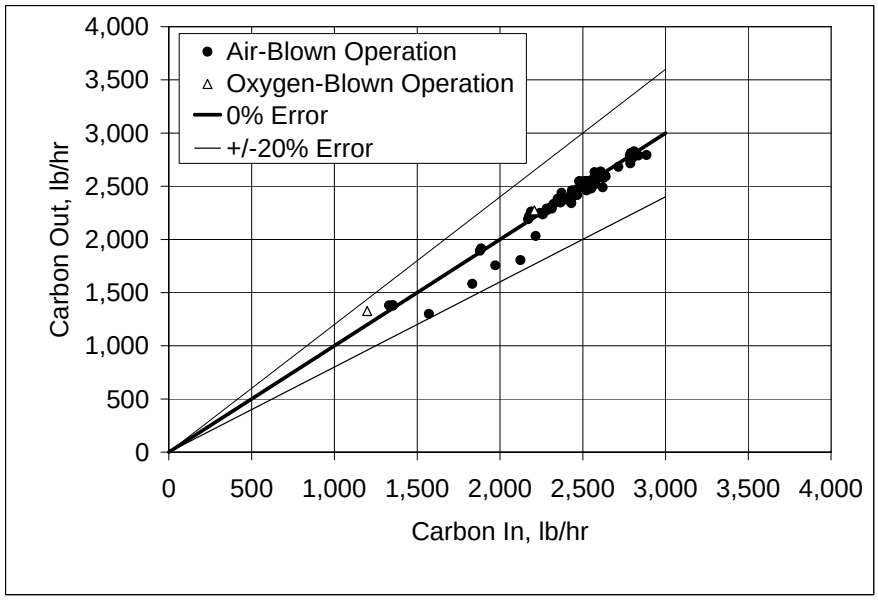

Figure C-3. Carbon Balance.

APPENDIX D LIST OF ABBREVIATIONS AND UNITS

Abbreviations

CCAD—Continuous Coarse Ash Depressurization
CFAD—Continuous Fine Ash Depressurization
DOE—Department of Energy
FEAL—Iron Aluminide
FTIR—Fourier Transform Infrared
GCT—Gasification Commissioning Test
GTI—Gas Technology Institute
HHV—Higher Heating Value
IGCC—Integrated Gasification Combined Cycle
LMZ—Lower Mixing Zone
LOI—Loss on Ignition
MMD—Mass Median Diameter
PCD—Particulate Control Device
PDI—Pressure Differential Indicator
PPC—Process Particle Counter
PRB—Powder River Basin
PSDF—Power Systems Development Facility
SMD—Sauter Mean Diameter
SRI—Southern Research Institute
TC—Test Campaign

Units

Btu—British thermal units
^{o}F—degrees Fahrenheit
ft—feet
ft^3—cubic feet
g/cm^3 or g/cc—grams per cubic centimeter
hr— hours
inH_2O—inches of water
in—inches
inwc—inches of water column
lb—pounds
min—minutes
mm—millimeters
MMBtu—million British thermal units
mol—mole
µm—microns or micrometers
MW—megawatts
ppm—parts per million
ppmv—parts per million by volume
ppmw—parts per million by weight
psi—pounds per square inch
psig—pounds per square inch gauge
s or sec—second
SCF—standard cubic feet
wt—weight